

QUANTUM INFORMATION SCIENCE FROM THE PERSPECTIVE OF A DEVICE AND MATERIALS ENGINEER

S. Bandyopadhyay
Department of Electrical Engineering
Virginia Commonwealth University
Richmond, VA 23284
E-mail: sbandy@vcu.edu
Tel: 1+ (804) 827-6275
Facsimile: 1+ (804) 828-4269

Abstract

This chapter presents a bird's eye view of the rapidly burgeoning field of quantum information science. It is intended for a materials scientist, an electrical engineer in the solid state subdiscipline, or a condensed matter physicist. Four areas of quantum information science are discussed: quantum computing, quantum cryptography, quantum teleportation and quantum memory. Emphasis is placed on the first sub-area since that is where materials science and condensed matter physics is expected to have the strongest impact.

1 Introduction

Quantum mechanics plays a daily role in our lives. Everything that works - from the television screen to our brain - draws upon the laws of quantum mechanics. Little wonder therefore that quantum mechanics can play a central role in fashioning computing machinery. The idea of using quantum mechanics to build “quantum computers” that outpace “classical computers” is not all that new. The ideas have been around for more than 25 years. It is only recently that this field has received widespread attention as a result perhaps of rapid advances in device and materials technology, particularly nanotechnology. It is not all that difficult anymore to construct solid state devices where the quantum mechanical wave nature of electrons is manifested at a relatively balmy temperature of 77 K, the temperature of liquid nitrogen. It therefore behooves the device physics community to seriously ponder the art and science of quantum informatics.

What then is quantum informatics? Examples are always better than precepts and therefore it is easiest to grasp the nature of quantum computing by looking at some examples.

In classical digital computing (analog computing is another matter; it is not much used anyway), one is accustomed to the idea of representing numbers with binary bits and then manipulating the bits according to a given set of instructions (the program) to carry out a computation. A binary

bit is the most primitive carrier of information. It can have two values: 0 or 1. The information content of the bit is its value.

In the 1930s, there was an ongoing effort to identify a *mathematical* model of the computing process which will be independent of how the computer (hardware and software) is implemented. Alan Turing, Alonzo Church, Kurt Gödel and Emil Post, independently developed mathematical models of computation that were independent of any assumptions regarding how the computer is built. Gödel identified algorithmic (computation) processes with general recursive functions (functions that call themselves). Church identified them with the so-called the λ -definable functions [1]. Turing, on the other hand, provided a very physical picture. He visualized the computing process as the actions of a so-called universal Turing machine. It consists of an infinite tape and a head. The tape has an infinite sequence of bits. The head can reset any bit to 0 or 1, reset its own internal memory, and then jump one bit to the left or right, or simply stay where it is. This machine can execute any classical algorithm and therefore model any classical computer [2].

It has now been shown that Gödel's, Church's and Turing's models are all equivalent. Roman Maeder [3] has written a simulator showing how the computation of any recursive function, that calls itself, can be simulated in a deterministic Turing machine, thereby unifying Gödel's model directly with Turing's.

There are two classes of Turing machines: deterministic and probabilistic. We will discuss them briefly.

1.1 Deterministic Turing machines

The deterministic Turing machine consists of an infinitely long tape partitioned into cells, each containing a 0, or a 1. There is a read/write head that can move left or right by one cell at a time. The head can exist in one of a finite set of memory states and contains a set of instructions (a program) that specify, depending on the current internal state and the bit currently being read by the head, how the internal state of the head will change, whether the bit being scanned will be changed and in which direction the head will move, if it moves at all.

The so-called Church-Turing thesis states that any computation can be modeled by the universal Turing machine. This thesis is the cornerstone of computer science and its implication is profound. This means that expensive supercomputers with several parallel processors and inexpensive personal computers, are, in a sense, equally powerful. They are both described by the universal

Turing machine. Given enough memory and time, the personal computers can do anything that supercomputers can.

1.2 Probabilistic Turing machines

While the head of a deterministic Turing machine, in a given state, reading a certain bit on the tape, has only one (unique) successor state available to it, a probabilistic Turing machine has multiple successor states available. Which state is ultimately acquired depends on a random choice. It is obvious then, that the probabilistic machine does not produce the correct answer with absolute certainty. If one requires a correct answer with absolute certainty, then there is an uncertainty in the length of time the probabilistic Turing machine must run. In fact, there is a trade-off between the time it takes to produce an answer and the probability that the answer is correct. Curiously, many problems can be solved more efficiently on a probabilistic Turing machine than on a deterministic Turing machine using the so-called random algorithms. It has been shown that anything computable by a probabilistic Turing machine is computable by a deterministic Turing machine and vice versa, although the probabilistic machine may be more efficient in some cases [4].

2 Quantum Turing machines

Despite the immense success of the universal Turing machine in modeling computation, it has one serious shortcoming. It is really not completely universal since it is now understood that it is not completely independent of the physical model of the computer. Perhaps unknowingly, Turing based his machine on the models of the classical world. The Turing machine is unable to capture the subtleties of the quantum mechanical world and computation processes based on quantum mechanics. There is now a model of *Quantum Turing machines*. It has a long history and started with Charles Bennet first showing that there exists a *reversible Turing machine* such that if the state of the machine is known at any time, it is possible to predict the states at all future times and all past times. There is no dissipation and loss of information in this machine [5].

Bennet's reversible Turing machine was completely classical, but it portended a quantum mechanical sister since the dynamical evolution of an isolated quantum system is also completely reversible in time. In 1980, Paul Benioff devised a quantum system whose actions mimicked that of a classical reversible Turing machine [6]. Benioff's machine was not a true quantum Turing

machine however, since although in between computation steps the machine existed in a quantum mechanical state, it reverted to a classical state at the conclusion of each computation step. Thus, this machine was no more powerful than Bennel’s classical reversible Turing machine.

In 1982, Richard Feynman showed that no classical Turing machine could simulate quantum phenomena without an exponential penalty in processing time [7]. Finally, in 1985, David Deutsch devised the first true quantum Turing machine. Its read, write and move operations were executed via quantum mechanical interactions. More importantly, whereas a classical Turing machine (including the reversible one) could encode only a 0 or a 1 in each cell of the tape, the quantum machine could encode a *superposition* of 0 and 1 simultaneously in each cell. Thus, the quantum machine could encode many inputs simultaneously on the same tape and perform a calculation on all of them in one step, completing the calculation in the time it takes for a classical machine to do the calculation on only one of the inputs. This immense speed up is called *quantum parallelism*. More on it later.

3 Qubits

To understand quantum parallelism, and indeed to understand the nuances of quantum computing, one must first understand the concept of quantum bits (or “qubits”).

Quantum computing does not process classical bits. Instead, it processes quantum bits (or “qubits”) which are neither 0 or 1, but a coherent superposition of both 0 and 1. This means that the bit is neither 0, nor 1, which does not make sense classically, but makes perfect sense quantum mechanically. The qubit can be written as

$$qubit = a_0|0 \rangle + a_1|1 \rangle \tag{1}$$

where $|0 \rangle$ denotes the state in which the qubit has a value of 0 and $|1 \rangle$ denotes the state in which the qubit has a value of 1. The coefficients a_0 and a_1 are complex quantities whose squared magnitudes denote the probability that if a measurement is performed on the qubit, it will be found to have a value of 0 and 1 respectively. Note that although a qubit can exist in suspended animation – between a 0 and a 1 – it must ultimately succumb to the fate of having a definite classical value (0 or 1) when it is “measured”. The outcome of the measurement is unambiguous. However, prior to the measurement, the qubit is neither 0, nor 1. It is in a so-called coherent superposition state,

and the measurement can yield a value of either 0 or 1. All we can say is that the probabilities of getting those two values are respectively $|a_0|^2$ and $|a_1|^2$. Note also that since the measurement can yield a value of only 0 or 1, and nothing else, it follows that

$$|a_0|^2 + |a_1|^2 = 1 \quad (2)$$

We emphasize that Equation (1) *does not* imply that the qubit is sometimes in state $|0\rangle$ with probability $|a_0|^2$, and the rest of the time in state $|1\rangle$ with probability $|a_1|^2$. It is only after measurement that the qubit collapses to a classical bit and assumes a definite value of 0 or 1. Prior to the measurement, it *does not* have a definite value; it is both 0 and 1, *all the time*. It is therefore called a superposition state.

While one can easily understand the meaning of “superposition” from the foregoing discussion, to understand the implication of a “coherent” superposition requires a little more reflection. Coherence has to do with the phases of a_0 and a_1 (being complex quantities, they have an amplitude and a phase). It might appear that the phase is never relevant since these coefficients seemingly determine only the probabilities which, in turn, depend only on the squared magnitudes. This is actually not true. Consider a hypothetical bit-flip operator \hat{O}_{flip} whose action is to flip a bit from 0 to 1 and vice versa (a classical realization of a bit flip operator is an inverter or NOT gate). Its action on a bit can be represented as

$$\begin{aligned} \hat{O}_{flip}|0\rangle &= |1\rangle \\ \hat{O}_{flip}|1\rangle &= |0\rangle \end{aligned} \quad (3)$$

Note from the above that $|0\rangle$ and $|1\rangle$ are not eigenstates of the operator. If we want to calculate the expected value of this operator for a system described by a qubit, we will get (following the usual prescription of quantum mechanics)

$$\begin{aligned} \text{expected value} &= \langle \text{qubit} | \hat{O}_{flip} | \text{qubit} \rangle \\ &= |a_0|^2 \langle 0 | \hat{O}_{flip} | 0 \rangle + |a_1|^2 \langle 1 | \hat{O}_{flip} | 1 \rangle + a_0 * a_1 \langle 0 | \hat{O}_{flip} | 1 \rangle + a_1 * a_0 \langle 1 | \hat{O}_{flip} | 0 \rangle \\ &= a_0 * a_1 + a_1 * a_0 \\ &= 2|a_0||a_1|\cos\theta \end{aligned} \quad (4)$$

where θ is the phase angle difference between a_0 and a_1 . In deriving the last equation, we used Equations (1) and (3) and also the fact that $|0\rangle$ and $|1\rangle$ are orthonormal states by themselves.

The fact that $|0\rangle$ and $|1\rangle$ are orthogonal to each other is obvious because any measurement outcome can produce either a 0 or a 1, and absolutely nothing in between. Thus the two possible outcomes are mutually exclusive, meaning that the two states are orthogonal to each other.

Equation (4) clearly shows that there are quantities that depend on the phases of a_0 and a_1 . Thus maintaining the correct phase relations between these quantities, or “coherence” is important. Quantum computation depends critically on this coherence.

Before ending this section, we point out that a_0 and a_1 are continuous (analog) variables whose magnitudes can take any value between 0 and 1 and whose phases can also take any value between 0 and 2π . On the other hand, the states $|0\rangle$ and $|1\rangle$ correspond to digital binary bits. Thus, quantum computation is neither quite analog computing, nor digital, but something in between.

4 Superposition states

We are now ready to provide the first glimpse of the power of quantum computing. Consider a bistable atom. We can use the excited state to encode the binary bit 1 and the ground state to encode the binary bit 0. Classically, this atom can store only one bit of information (whose value can be 0 or 1) because we have two degrees of freedom (ground and excited) and two possible values of the binary bit. Since each atom can store only one bit, N bistable atoms can store N binary bits classically. But now, if we can create a coherent superposition of the states of two atoms, the corresponding qubit will be written as

$$qubit_{2\text{ atom}} = a_{00}|00\rangle + a_{01}|01\rangle + a_{10}|10\rangle + a_{11}|11\rangle \quad (5)$$

where the state $|ij\rangle$ corresponds to the first atom being in state $|i\rangle$ and the second atom in state $|j\rangle$. This system can, in principle, store 2^2 bits of information corresponding to (i) both atoms being in the ground state, (ii) first in ground state and second in excited, (iii) first in excited and second in ground, and (iv) both excited. Note that the classical case would correspond to only one of the coefficients in Equation (5) being non-zero. Extending this to N bistable atoms, we can write the corresponding qubit as

$$qubit_{N\text{-atom}} = \sum_{x_1 x_2 \dots x_N} a_{x_1 x_2 \dots x_N} |x_1 x_2 \dots x_N\rangle \quad (6)$$

where the x 's can take the value 0 or 1. The above equation has 2^N terms. It means that while N bistable atoms can store N binary bits classically, the same system can store 2^N classical bits

quantum mechanically. Here is the clincher. If we want to store 2^{1000} binary bits of information, it is impossible in the classical realm since the number 2^{1000} is larger than the number of atoms in the known universe. However, in the quantum mechanical realm, just 1000 bistable atoms in a coherent superposition state can do the job. These 1000 atoms could store more information than all the hard disks in the universe made over the life of the universe!

Now the tempered vision. One might be tempted to think that we can make a huge “memory” storing 2^N binary bits of information using just N bistable atoms. This point of view would be *incorrect*. A true memory should be such that every time it is accessed, it returns the *same* data which is stored in it. For instance, if we have stored the binary string 11001, we should get this string *every time* the memory is read. But the quantum memory we are talking about does not satisfy this requirement. Every time we read the memory, the qubits collapse to classical bits and we only get N (not 2^N) bits out of it. More importantly, the values of these bits change with each measurement because of the probabilistic nature of quantum measurement. It is never the same bit string in two successive measurements! Surely, this cannot be judged a reliable memory. There is a subtle difference between *memory* and *storage*. Memory implies accessibility and fidelity, storage does not. We may store 2^N bits of information, but not be able to access them. However, the ability of the quantum system to co-exist in 2^N states is what is important. It forms the basis of an attribute known as quantum parallelism.

5 Quantum Parallelism

In the world of classical computers, parallelism refers to parallel (simultaneous) processing of different information in different processors. Quantum parallelism refers to simultaneous processing of different information or inputs in the *same* processor. This idea, due to Deutsch, refers to the notion of evaluating a function once on a superposition of all possible inputs to the function to produce a superposition of outputs. Thus, all outputs are produced in the time taken to calculate one output classically. Of course, not all of these outputs are accessible since a measurement on the superposition state of the output will produce only one output. However, it is possible to obtain certain joint properties [9] of the outputs, and that is a remarkable possibility.

Let us exemplify quantum parallelism more concretely. Consider the situation when N inputs x_1, x_2, \dots, x_N are provided to a computer and their functions $f(x_1), f(x_2), \dots, f(x_N)$

are to be computed. The results are then fed to another computer to calculate the functional $F(f(x_1), f(x_2), \dots, f(x_N))$.

With a classical computer, we will calculate $f(x_1), f(x_2), \dots, f(x_N)$ serially, one after the other. With a quantum computer, the story is different.

Prepare the initial state as a superposition of the inputs.

$$|I\rangle = \frac{1}{\sqrt{N}}(|x_1\rangle + |x_2\rangle + \dots + |x_N\rangle) \quad (7)$$

Let it evolve in time to produce the output

$$|O\rangle = \frac{1}{\sqrt{N}}(|f(x_1)\rangle + |f(x_2)\rangle + \dots + |f(x_N)\rangle) \quad (8)$$

Note that $|O\rangle$ has been obtained in the time required to perform a single computation. Now, if $C = F(f(x_1), f(x_2), \dots, f(x_N))$, can be computed from $|O\rangle$, then a quantum computer will be of great advantage. This is an example where “quantum parallelism” can be used to speed up the computation tremendously.

There are two questions now. Can C be computed from a knowledge of the superposition of various $f(x_i)$ and not the individual $f(x_i)$ s? The answer is “yes”, but for a small class of problems. These are called the Deutsch-Josza class of problems which can benefit from quantum parallelism. Second, can C be computed correctly with unit probability. The answer is “no”. C cannot be computed with unit probability. However, if the first answer is wrong (hopefully, the computing entity can differentiate right from wrong answers), then the experiment or computation is repeated until the right answer is obtained. The probability of getting the right answer within k iterations is $(1 - p^k)$ where p is the probability of getting the wrong answer in any iteration. The mean number of times the experiment should be repeated is $N^2 - 2N - 2$.

The following is an example of Deutsch-Josza class of problems. For integer $0 \leq x \leq 2L$, given that the function $f_k(x) \in [0,1]$ has one of two properties – (i) either $f_k(x)$ is independent of x , or (ii) one half of the numbers $f_k(0), f_k(1), \dots, f_k(2L - 1)$ are zero – determine which type the function belongs to using the fewest computational steps.

The most efficient classical computer will require $L+1$ evaluations, whereas according to Deutsch and Josza, a quantum computer can solve this problem with just two iterations.

6 Classical and Quantum Complexity

In computer science, complexity refers to how efficiently a problem can be solved. A measure of the efficiency is the rate of growth of the time or memory required to solve a problem as the size of the problem increases. Complexity measures are independent of the make and prowess of the computer, but depend on the mathematical model of the computer, such as whether it is a deterministic classical Turing machine, a probabilistic classical Turing machine, or a quantum machine. In fact, many problems that are deemed intractable on a deterministic classical Turing machine can be solved very efficiently with high probability of success on a probabilistic classical Turing machine. In classical complexity theory, there are 5 classes of problems [12]. They are shown in Table 1.

The study of quantum complexity classes begun with Deutsch [8]. Since the quantum Turing machine is a quantum mechanical refinement of probabilistic Turing machines, the quantum complexity classes are close cousins of the probabilistic complexity classes. There are three known quantum complexity classes [12] which are shown in Table 2.

6.1 History of quantum complexity theory

Deutsch's idea of quantum parallelism [8] was an interesting concept, but certainly did not establish the superiority of quantum computers over classical computers. With quantum computers, even though one could, in principle, calculate the outputs corresponding to all possible inputs in one go, when the final answer is read, only one of the outputs is obtained since the superposition state (wave function) collapses to a classical state under the read operation which constitutes a measurement. Worse still, all the other outputs are permanently lost.

In 1992, Deutsch and Josza [10] contrived a problem that a deterministic Turing machine could solve in linear time, but a quantum Turing machine solved in a time that was a polynomial in the logarithm of the problem size. Thus, the quantum machine was exponentially more efficient than the deterministic machine. However, the probabilistic machine was equally efficient as the quantum machine and hence the superiority of the quantum over the classical was still elusive.

The following year, Bernstein and Vazirani came up with the first problem where the quantum Turing machine beat *both* the probabilistic and the deterministic classical Turing machines. The

Table 1: Classical complexity classes

Class	Description	Example
P	The running time of the algorithm is a polynomial in the size of the input	Division, addition
NP	Non-deterministic polynomial running time	Factoring integers
NP-complete	A subset of problems in NP that can be mapped into one another in polynomial time. If one of the problems is tractable, they all are	Traveling salesman problem
ZPP	Can be solved with certainty by probabilistic Turing machines in polynomial time on the average	
BPP	Can be solved in polynomial time with probability of correctness $> 2/3$	

Table 2: Quantum complexity classes

Quantum Class	Description	Comparison with Classical
QP	The running time of the algorithm is a polynomial in the size of the input and the problem can be solved with certainty	P is included in QP. Quantum computer can solve more problems in polynomial time than its classical counterpart
BQP	Can be solved in polynomial running time with probability of success $> 2/3$	For this class, quantum machines are at least as powerful as classical ones. It is not known if they are more powerful
ZQP	Can be solved with zero error probability in polynomial time	ZPP is included in ZQP. Quantum computers can solve more problems in this class than classical computers

problem was to sample from the Fourier spectrum of a Boolean function of n bits.

The crowning achievement in this area was the work of Peter Shor [11] who discovered a polynomial time algorithm for factoring large integers. This is the first problem of great practical significance that a quantum computer can solve in polynomial time (in classical complexity class, this is an NP problem). The practical significance is associated with breaking secure cryptographic codes. Many cryptosystems are based on *trapdoor functions*. These are functions that are easy to compute, but their inverse is difficult to compute. The best example is the following. It is relatively easy to find the product of two large prime integers (multiplication is in the complexity class P), but the reverse process of factorizing the product back into two prime integers is unbelievably difficult (it is in the class NP). Williams and Clearwater, in their very popular book on quantum computing, give the following example [12]. Consider two prime numbers 15485863 and 15485867. Multiplying these numbers by hand using pen and paper took this author a few minutes to produce the product 239812014798221. The author would not have been able to factorize the product back into the prime factors in his lifetime (of course, he would have run out of patience long before his life ended).

What is true of humans is also true of computers. The most popular classical algorithm for factoring is the Multiple Polynomial Quadratic Sieve for numbers with 100-150 decimal digits [13]. The running time of this algorithm grows sub-exponentially, but super-polynomially in time. In 1978, Rivest, Shamir and Adelman challenged computer scientists to factorize an integer consisting of 129 digits. The challenge was finally met in 1994 by a team of computer scientists using over 1500 networked computers. Crandall has estimated that this task would require a computer executing 1 millions instructions per second, 5000 years to compute [14].

Trapdoor functions are ideal for use in cryptosystems. Suppose I want to transmit a secret message to my friend and I encode the message in the prime number 15485863 using a publicly known encryption method. I have also provided my friend with the prime number 15485867 as a “key” ahead of time. I then transmit the *product* of the message and the key - in this case, the number 239812014798221 - over a public channel to my friend. For me, multiplying the two numbers and checking their primality takes very little time. Upon receipt, my friend divides his key into the number 239812014798221 and extracts the actual message 15485863 quite easily. An eavesdropper who does not have the key gets only the number 239812014798221 and has to factorize it into its prime constituents. That is hard and takes much longer than the period over which the

message has any usefulness to the eavesdropper.

This, of course, is a very primitive cryptosystem. There are more sophisticated cryptosystems such as the RSA scheme devised by Rivest, Shamir and Adelman [15]. It is similar in spirit to what was just described and relies on the difficulty of factorization for security. Hence, the development of an algorithm that can factorize large numbers in polynomial times threatens the security of many of our most advanced cryptosystems. Hence, Shor's algorithm is a very important advance.

Shor's algorithm relies on a result from number theory that establishes a relationship between the period of a particular periodic function to the factors of an integer. Let us say that we wish to factorize an integer n . We will construct a function $\phi_n(x) = r^x \text{mod}(n)$ where r is an integer chosen at random that is co-prime to n , meaning that the greatest common divisor of r and n is 1. As we increase the argument x of the function $\phi_n(x)$ in steps, taking $x = 0, 1, 2, ..$ etc., the function $\phi_n(x)$ ultimately fall into a periodic pattern. The period can be used to find the factors of n efficiently, but there is unfortunately no efficient classical algorithm to find the period in the first place. Shor's contribution was to develop a quantum algorithm for finding this period efficiently. His technique relies on quantum parallelism to find the period of the function $\phi_n(x)$ rather quickly. Another factorizing algorithm for quantum computers has been proposed by Kitaev [16].

Similar ideas have been used to solve another problem, namely database search. Grover [17] has discovered an algorithm for finding a single item in an unsorted database in square root of the time it will take on a classical computer. These ideas have been extended to find the minimum [18] of the database as well, more efficiently than any classical computer can.

Unfortunately, at this time, there are only *two* classes of algorithms - factorizing and searching databases - where quantum computers evince an edge. No significant advancement has been made in finding other classes of algorithms over the last five years, to the best of the author's knowledge. Since the field is so new, there is hope however that rapid advances may be around the corner.

7 The early history of quantum information science: reversible computers

Quantum computing has interesting roots. Its progenitor, reversible computing, itself has a long history and is extremely relevant to today's nanoelectronics. There is a long standing belief in the device research community that the silicon steamroller, that paved the way for the microelectronics

revolution, will ultimately run out of steam. Future silicon CMOS may encounter insurmountable problems due to excessive power dissipation, breakdown of scaling laws and certain fundamental limits imposed by the laws of quantum mechanics. While the fundamental limits are still a moot issue, excessive power dissipation is universally acknowledged to be a serious problem. Microelectronic logic gates of present-day vintage dissipate about 0.1 pJ of energy per switching cycle. The Semiconductor Industry Association's National Technology Roadmap projects that by the year 2007, the dynamic power dissipated in CMOS devices will be 600 nW per logic gate with a gate density of $5 \times 10^7 / \text{cm}^2$, corresponding to a dissipation of 30 W/cm^2 of chip area [19]. ¹ Fifteen years ago, removal of 1000 W/cm^2 was demonstrated in a silicon chip [20]. Unfortunately, heat sinking technology is not keeping pace with solid state circuits technology and excess heat removal will soon be a problem. Consequently, it appears that at least in the near future, the gate density may be constrained to $10^{10} \text{ gates/cm}^2$ from mere heat sinking considerations. Any denser device density will require either more efficient heat removal techniques, or less power dissipation per logic gate. It is the latter objective that has captured the imagination of device physicists.

In a seminal paper published in 1961 [21], Rolf Landauer addressed the fundamental issue of dissipation and showed that the minimum energy that must be dissipated in a single *logically irreversible* bit operation is $kT \ln 2$ (k = Boltzmann constant and T = absolute temperature of the logic device) which is about 4×10^{-21} Joules at room temperature (see Section 7.1 for a derivation). We will explain "logical irreversibility" later, but first note that this figure is far smaller than what CMOS or single electron transistors [22] will dissipate in a logic bit operation by the year 2007. However, the very existence of this figure portends a practical limit to downscaling of conventional logic circuits. Assuming that the most advanced devices, constrained only by the Landauer limit, will switch in 1 picosecond, the power dissipated will be 4 nW/gate. Moreover, assuming that heat sinking technology will allow removal of only 10 kW/cm^2 , the gate density will saturate to $2.5 \times 10^{13} \text{ gates/cm}^2$ unless dramatic improvements in heat sinking are achieved. The alternative is to seek ways to circumvent the $kT \ln 2$ barrier.

Before we address ways of overcoming the $kT \ln 2$ barrier, we need to derive the existence of this barrier first because it will also show us how we can circumvent it.

¹A good toaster oven dissipates only about 100 W/cm^2 . None of this is of course removed. It is used to toast bread and bagels.

7.1 Derivation of the “ $kT\ln 2$ ” limit

From simple thermodynamics, the energy dissipated when a system is switched from one state to another is

$$\Delta E = k(T\Delta S + S\Delta T) \quad (9)$$

where k is the Boltzmann constant, T is the absolute temperature and S is the system’s entropy.

The entropy is given by

$$S = \sum_i p_i \ln(p_i) \quad (10)$$

where p_i is the probability of the system to be in the i -th state. For a binary device, there are only two states ($i = 0,1$).

Let us consider a device which is switched. Prior to switching, it had equal probability of being in the state 0 and 1. Therefore, its initial entropy is

$$S_{initial} = p_0 \ln(p_0) + p_1 \ln(p_1) = 0.5 \ln(0.5) + 0.5 \ln(0.5) = -\ln 2 \quad (11)$$

After switching, we can measure the final state and know for sure whether the system is in state 0 or 1. Let us say that we find it is in state 1. Then,

$$S_{final} = 0 \ln(0) + 1 \ln(1) = 0 \quad (12)$$

Therefore, the change in entropy is

$$\Delta S = S_{final} - S_{initial} = \ln 2 \quad (13)$$

For an isolated system $\Delta T \geq 0$. Substituting all this in equation 9 yields

$$\Delta E_{min} = kT \ln 2 \quad (14)$$

7.2 Physical and logical irreversibility

This derivation tells us a lot. Initially, the system could have been in either state 0 or 1. Later we found out that it was in the 1 state. This constricts the phase space for the system’s state (decreases the number of possibilities) and causes dissipation. The entropy is raised when we constrict the phase space in this fashion. But what if we could always deduce unambiguously what the initial state was from a measurement of the final state? In that case, the initial state also has only one possibility, not two. Consequently, we would not have constricted the phase space and would have

caused no dissipation. It is easy to see from our derivation that in this case $S_{initial} = S_{final} = 0$. Therefore, $\Delta S = 0$ and $\Delta E_{min} = 0$. To avoid dissipation, the trick is to ensure that if we *reverse* the system in time, it ends up in a *unique* state. Such a system is said to be time reversible, and therefore dissipationless. Dissipation accrues from time irreversibility, and time irreversibility is also called physical irreversibility.

Landauer’s seminal contribution was to connect physical irreversibility to *logical irreversibility* and vice versa. This connection can be visualized better with a concrete example pointed out to the author by a colleague [23]. Consider two parabolic wells (Fig. 1). One has walls that are frictionless and the other has normal walls with friction. A marble rolls along both walls. If we know the position and velocity of the marble in the frictionless well at any given time, we can always determine the position and velocity at any *previous* instance of time using Newton’s laws which are reversible in time. But in the other well, the final position of the marble (after a long enough time has elapsed) is always at the bottom and the final velocity is always zero, *regardless of the initial position and velocity*. The second well has dissipation due to friction and hence we cannot deduce the initial state from the final state. If the position and velocity are considered as logic variables, the well will be a logic gate, the initial and final states will be inputs and outputs. Then, the second well is logically irreversible and causes dissipation. The first well is logically reversible and causes no dissipation.

7.3 Reversible and irreversible gates

There is a great deal of interest in classical, but reversible, gates since these gates can overcome the $kT \ln 2$ barrier and be dissipationless. Irreversible gates, on the other hand, must dissipate at least $kT \ln 2$ amount of energy per bit operation.

Let us look at some examples of (classical) logically reversible and logically irreversible gates. Consider the simplest AND gate with two inputs and one output whose truth table is given below

Input 1	Input 2	Output
0	0	0
0	1	0
1	0	0
1	1	1

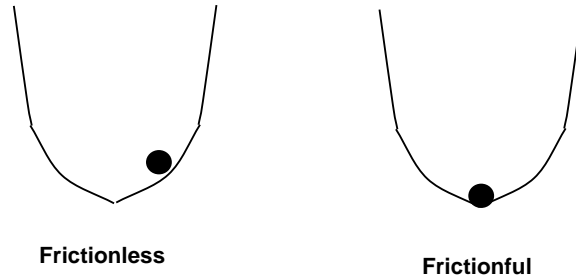


Figure 1: Two wells, one frictionless and the other is not. A marble rolls along the walls. Knowing the position and momentum of a marble in the frictionless well at any instant of time allows us to compute the position and momentum at all future and past time. However, for the well with friction, the final position of the marble is always at the bottom and it is at rest. We cannot predict from the final position and momentum what the initial position and momentum were.

If the output is 1, we can confidently state that the inputs were both 1. However, if the output is 0, then we cannot state what the inputs were since there are three sets of possibilities. Because we cannot deduce the inputs unambiguously from the output alone - there is no unique relation between the two - this is a logically irreversible gate. On the other hand, it is obvious that an inverter is a logically reversible gate. There is a unique relation between the input and the output; one is always the logic complement of the other. Therefore, if we know one, we always know the other.

There is another (mathematical) way to view this. An inverter converts a 0 to a 1 and vice versa. Thus, the 2×2 matrix operator relating an input vector to the output vector (the vectors span the Hilbert spaces of the inputs and outputs) is given by the relation:

$$\begin{array}{c} \left[\begin{array}{c} 0 \\ 1 \end{array} \right] \\ \text{output} \end{array} = \begin{array}{c} \left[\begin{array}{cc} 0 & 1 \\ 1 & 0 \end{array} \right] \\ A - \text{matrix} \end{array} \begin{array}{c} \left[\begin{array}{c} 1 \\ 0 \end{array} \right] \\ \text{input} \end{array} \quad (15)$$

The matrix operator for a logic gate is called an A-matrix. For an inverter, or for that matter any logically reversible gate, the A-matrix must be invertible and its determinant must not vanish. It

also stands to reason that a reversible gate must have as many outputs as inputs.

7.4 Universal reversible gate

Anybody somewhat familiar with classical Boolean logic circuits knows that there are two primitive gates that are “universal” in the sense that any arbitrary logic circuit can be built by using just (either one of) those gates alone. They are the NAND gate and the NOR gate. A fundamental theorem of Boolean algebra is that any Boolean function can be completely re-written in terms of NAND or NOR functions. Therefore, any Boolean combinational circuit can be built with just NAND or NOR gates.

Neither the NAND, nor the NOR gate is however reversible. So the question is: are there universal reversible gates and if so, what are they? One universal reversible gate is the Toffoli-Fredkin gate [24]. It has 3 inputs (a, b, c) and 3 outputs (a', b', c') (remember that the number of inputs and outputs have to be equal for a reversible gate). The Toffoli-Fredkin (T-F) gate is a universal gate in the sense that any reversible computation can be achieved by repeated operations of the T-F gate. In other words, any reversible combinational circuit can be built by connecting T-F gates. The truth table of a T-F gate is

a	b	c	a'	b'	c'
0	0	0	0	0	0
0	0	1	0	0	1
0	1	0	0	1	0
0	1	1	0	1	1
1	0	0	1	0	0
1	0	1	1	0	1
1	1	0	1	1	1
1	1	1	1	1	0

The above truth table indicates that the input-output relation of the T-F gate is such that $a' = a$, $b' = b$, $c' = c \oplus a \cdot b$ (where \oplus denotes the exclusive OR Boolean function and the “dot-product” denotes the Boolean AND function). The variables a and b are called control bits and the variable c is the target bit. The control bits pass through the gate without change. The target

bit is flipped only if both control bits are logical 1.

We wrote the A-matrix of the basic 1-bit inverter in Equation 15 using the computational basis states $|0\rangle$ and $|1\rangle$. We can write an A-matrix for the 3-bit T-F gate using the 3-bit computational basis states $|000\rangle$, $|001\rangle$, $|010\rangle$, $|011\rangle$, $|100\rangle$, $|101\rangle$, $|110\rangle$, and $|111\rangle$ (here the basis states are possible values of $|abc\rangle$):

$$A_{Tofoli-Fredkin} = \begin{bmatrix} 1 & 0 & 0 & 0 & 0 & 0 & 0 & 0 \\ 0 & 1 & 0 & 0 & 0 & 0 & 0 & 0 \\ 0 & 0 & 1 & 0 & 0 & 0 & 0 & 0 \\ 0 & 0 & 0 & 1 & 0 & 0 & 0 & 0 \\ 0 & 0 & 0 & 0 & 1 & 0 & 0 & 0 \\ 0 & 0 & 0 & 0 & 0 & 1 & 0 & 0 \\ 0 & 0 & 0 & 0 & 0 & 0 & 0 & 1 \\ 0 & 0 & 0 & 0 & 0 & 0 & 1 & 0 \end{bmatrix} \quad (16)$$

The A-matrix is not diagonal, but it is obviously unitary. The unitarity guarantees reversibility.

Lloyd has proposed an experimental realization of the T-F gate [25]. Consider three bistable atoms A , B and C . The excited states encode the binary bit 1 and the ground states the binary bit zero. The energy separation between the excited and ground state of atom C depends on whether the atoms A and B are both excited or not. An electromagnetic pulse (called a π -pulse) is applied to the 3-atom system which is resonant with the energy separation between the excited and ground states of atom C when both A and B are in excited states. This pulse will flip atom C from excited to ground state (or vice versa), thereby realizing the operation of a T-F gate. A quantum dot realization of a T-F gate, based on an exact calculation of the dependence of the energy separation between the excited and ground states of C on the states of A and B has been reported by us [33].

There is a vast body of work dedicated to different implementations of reversible (dissipationless) gates using various physical systems. Some are mechanical in nature such as billiard balls, some are electrical, some optical and yet some others are chemical. The first generation of these “dissipationless” systems comprised logically reversible gates that dissipate less than $kT \ln 2$ amount of energy (but not necessarily zero energy) per bit flip. Concrete proposals for such systems were advanced by Bennett [26, 27], Toffoli [28], Fredkin [24], Likharev [29] and Landauer [30] among others. None of these proposals envisioned nanoelectronic (or even semiconductor solid-state) im-

plementation. Only recently, nanoelectronic versions based on single electron parametron [31], two-level atoms or molecules [25], and Coulomb or exchange-coupled quantum dots [32, 33] have appeared in the literature.

8 Quantum gates

Quantum gates are of course always reversible in nature since they rely on the quantum mechanical evolution of a system to operate on qubits. The quantum mechanical evolution is described by the Schrödinger equation which obeys time reversal symmetry. All quantum mechanical evolutions are unitary in that the wave function $\psi(t)$, at any time t , is related to the wave function $\psi(0)$ at time $t = 0$, by the relation

$$\psi(t) = e^{-iHt/\hbar}\psi(0) \tag{17}$$

where H is the Hamiltonian of the system and a Hermitean operator. Therefore the operator $e^{-iHt/\hbar}$ is unitary.

8.1 The strange nature of quantum gates

Quantum gates are strange entities that may not have any classical analog. Let us say that we want to invert a classical bit by operating with an ordinary *NOT* gate. We choose to do this by operating on the input bit with two strange gates in succession that we call “square-root-of-NOT” gates denoted by \sqrt{NOT} . The name comes about from the fact that the successive operation of two gates can be represented mathematically as the scalar product of their A-matrices. Thus, the logic operation that we are after can be written as

$$\sqrt{NOT} \cdot \sqrt{NOT} \equiv NOT \tag{18}$$

What makes this gate “quantum” (or at least non-classical) is that it is impossible to have a single-input/single-output classical binary gate that works in this fashion [12]. If the \sqrt{NOT} gate were classical, it should have an output of 0 or 1 for each possible input of 0 or 1. Suppose that we define the action of a \sqrt{NOT} gate as the pair of transformations

$$\begin{aligned} \sqrt{NOT}_{classical}(0) &= 0 \\ \sqrt{NOT}_{classical}(1) &= 0 \end{aligned} \tag{19}$$

Then, two consecutive applications of this gate will invert a 1 successfully, but not a 0, thereby violating Equation 18. We can try any other transformation:

$$\begin{aligned}\sqrt{NOT}_{classical}(0) &= 0 \\ \sqrt{NOT}_{classical}(1) &= 1\end{aligned}\tag{20}$$

This particular transformation does not invert any bit at all. In fact, it is impossible to define \sqrt{NOT} classically such that two successive operations of this gate will reproduce the behavior of a NOT gate.

The A-matrix of a \sqrt{NOT} gate can be defined as

$$A_{\sqrt{NOT}} = \begin{bmatrix} \frac{1+i}{2} & \frac{1-i}{2} \\ \frac{1-i}{2} & \frac{1+i}{2} \end{bmatrix}\tag{21}$$

Note that

$$\begin{bmatrix} \frac{1+i}{2} & \frac{1-i}{2} \\ \frac{1-i}{2} & \frac{1+i}{2} \end{bmatrix} \cdot \begin{bmatrix} \frac{1+i}{2} & \frac{1-i}{2} \\ \frac{1-i}{2} & \frac{1+i}{2} \end{bmatrix} = \begin{bmatrix} 0 & 1 \\ 1 & 0 \end{bmatrix}\tag{22}$$

so that $A_{\sqrt{NOT}} \cdot A_{\sqrt{NOT}} = A_{NOT}$, as required. Moreover, the matrix $A_{\sqrt{NOT}}$ is unitary which it must be.

Note that if a $A_{\sqrt{NOT}}$ gate is fed an input data string (0,1), it produces an output data string (α, β) given by

$$\begin{aligned}\alpha &= \frac{1+i}{2}|0\rangle + \frac{1-i}{2}|1\rangle \\ \beta &= \frac{1-i}{2}|0\rangle + \frac{1+i}{2}|1\rangle\end{aligned}\tag{23}$$

where the output bits are coherent superpositions of $|0\rangle$ and $|1\rangle$ which are qubits!. Thus, the $A_{\sqrt{NOT}}$ gate is a quantum gate.

The A-matrix in equation (1) is not the only A-matrix that can represent a \sqrt{NOT} gate. Consider the A-matrix

$$A_{\sqrt{NOT'}} = \frac{1}{\sqrt{2}} \begin{bmatrix} 1 & 1 \\ -1 & 1 \end{bmatrix}\tag{24}$$

This matrix is also a valid A-matrix for a \sqrt{NOT} gate since its square is the A-matrix of the NOT gate (never mind about the negative sign that you get when you operate the A-matrix twice

on the data string (0,1). In binary Boolean algebra, we will make no distinction between 1 and -1; the sign is unimportant). If this gate is fed an input data string (0,1), it produces an output data string (α', β') given by

$$\begin{aligned}\alpha' &= \frac{1}{\sqrt{2}}|1 \rangle + \frac{1}{\sqrt{2}}|0 \rangle \\ \beta' &= \frac{1}{\sqrt{2}}|1 \rangle - \frac{1}{\sqrt{2}}|0 \rangle\end{aligned}\tag{25}$$

which are also qubits (no surprise there).

Now a measurement of the output (either $|\alpha' \rangle$ or $|\beta' \rangle$) yields the answer 0 (state $|0 \rangle$) or 1 (state $|1 \rangle$) with equal probability $1/2$, yielding a *perfectly random* generator of bits 0s and 1s. A single computation with a single gate yields a perfectly random bit! This is an extension of “quantum parallelism”. First, a classical algorithm will require more than one gate and many computational steps to generate a random number. More importantly, the number will be *never truly random*. Mathematically, there is *no function* that generates a true random number (only pseudo-random numbers can be generated using algorithms). Thus, a classical Turing machine can only generate pseudo random numbers; it cannot generate a true random number. This also shows that the classical Turing machine is not really universal since it cannot model the quantum mechanical process of generating a true random number.

8.2 Universal quantum gates

The first universal quantum gate that was shown to be universal was not a 2-qubit gate, but rather a 3-qubit gate due to Deutsch. It is fashioned after the universal classical gate of Toffoli and Fredkin. Using the computational basis states $|000 \rangle$, $|001 \rangle$, $|010 \rangle$, $|011 \rangle$, $|100 \rangle$, $|101 \rangle$, $|110 \rangle$, and $|111 \rangle$, the A-matrix of the Deutsch gate is given by

$$A_{Deutsch} = \begin{bmatrix} 1 & 0 & 0 & 0 & 0 & 0 & 0 & 0 \\ 0 & 1 & 0 & 0 & 0 & 0 & 0 & 0 \\ 0 & 0 & 1 & 0 & 0 & 0 & 0 & 0 \\ 0 & 0 & 0 & 1 & 0 & 0 & 0 & 0 \\ 0 & 0 & 0 & 0 & 1 & 0 & 0 & 0 \\ 0 & 0 & 0 & 0 & 0 & 1 & 0 & 0 \\ 0 & 0 & 0 & 0 & 0 & 0 & A & B \\ 0 & 0 & 0 & 0 & 0 & 0 & B & A \end{bmatrix} \quad (26)$$

where

$$A = ie^{\frac{i\pi\alpha}{2}}(1 + e^{i\pi\alpha}) \text{ and } B = ie^{\frac{i\pi\alpha}{2}}(1 - e^{i\pi\alpha}) \quad (27)$$

and α may be an irrational number.

It is easy to check that $A_{Deutsch}$ is unitary. The T-F gate can be synthesized by connecting a number of Deutsch gates in series. The number of Deutsch gates required for this is N where N must satisfy the relation $[A_{Deutsch}]^N = A_{Toffoli-Fredkin}$. It is always possible to find an integer value of N as long as α is an irrational number. Noting that

$$\begin{bmatrix} ie^{\frac{i\pi\alpha}{2}}(1 + e^{i\pi\alpha}) & ie^{\frac{i\pi\alpha}{2}}(1 - e^{i\pi\alpha}) \\ ie^{\frac{i\pi\alpha}{2}}(1 - e^{i\pi\alpha}) & ie^{\frac{i\pi\alpha}{2}}(1 + e^{i\pi\alpha}) \end{bmatrix}^N = i^N e^{\frac{iN\pi\alpha}{2}} \begin{bmatrix} ie^{\frac{i\pi\alpha}{2}}(1 + e^{i\pi\alpha}) & ie^{\frac{i\pi\alpha}{2}}(1 - e^{i\pi\alpha}) \\ ie^{\frac{i\pi\alpha}{2}}(1 - e^{i\pi\alpha}) & ie^{\frac{i\pi\alpha}{2}}(1 + e^{i\pi\alpha}) \end{bmatrix} \quad (28)$$

the quantity $e^{iN\pi\alpha}$ can be made arbitrarily close to any complex number of unit norm by changing N . Choosing N such that $e^{iN\pi\alpha} = -1$ yields the Toffoli-Fredkin gate [35].

8.3 2-qubit universal quantum gates

Recently, it has been shown that there exist 2-qubit quantum gates which are universal. The proof of universality of these gates was given by DiVincenzo [36] using Lie algebra; however, it can also be shown that the Deutsch gate can be realized with these 2-qubit gates. This, in itself, is sufficient proof of universality. The Deutsch gate is not the most primitive universal quantum gate, the DiVincenzo gate is. Later, it was shown by Seth Lloyd that almost any 2-qubit gate is universal [37].

The computational basis of the 2-terminal (2 inputs and 2 outputs) universal quantum gate can be chosen as $|00\rangle$, $|01\rangle$, $|10\rangle$, $|11\rangle$. In this basis, the A-matrix of the universal 2-qubit gate is

$$A_{DiVincenzo} = \begin{bmatrix} 1 & 0 & 0 & 0 \\ 0 & 1 & 0 & 0 \\ 0 & 0 & A & B \\ 0 & 0 & B & A \end{bmatrix} \quad (29)$$

where A and B have been given by Equation 27.

9 Solid State Realizations of Quantum Gates

In 1996, this author and a co-worker proposed a simple spin based quantum inverter utilizing two exchange coupled quantum dots [32]. It is not a universal gate, but it relies on quantum mechanics to elicit the Boolean logic NOT function and is described below.

Consider two single electrons housed in closely spaced quantum dots as shown in Fig. 2. We will assume that there is only one size quantized level in each dot. A weak magnetic field H_z is applied globally to define a spin polarization direction. The ground state of this two-electron system is antiferromagnetic [38] with the two spins antiparallel (one spin will be aligned along the magnetic field and the other opposite to it). If spin polarization is used to encode binary bits such that up-spin represents binary bit 1 and down-spin binary bit 0, then the spin polarization of one electron is the logic complement of that of the other when the system is in ground state. This can be the basis of an inverter. We can orient the spin polarization in one dot (with a local magnetic field) to conform to the input bit and the output will automatically be the inverse of the input.

Let us study this system in a little more detail. Even a 2-electron system is quite complicated really when it comes to quantum mechanics. Any quantum system is described by a Hamiltonian which sums up the energy contributions to the electrons. The so-called Hubbard Hamiltonian for this system is

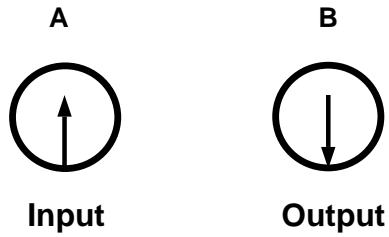


Figure 2: Two exchange-coupled electrons in two quantum dots A and B . The ground state of this system is anti-ferromagnetic; the spin orientation of one electron is anti-parallel to that of the other. If spin is used to encode logic bits, then this system acts as an inverter if we consider one quantum dot (A) as the input port and the other (B) as the output port. The spin orientation in A can be aligned by a SPSTM tip thus enabling a ‘‘write’’ operation. The spin orientation in B can be read by a SPSTM tip thus enabling a ‘‘read’’ operation. The same system can act as a quantum inverter since the ground state wave function is an entangled state and each quantum dot can exist in a coherent superposition of ‘‘upspin’’ and ‘‘downspin’’ states. Reproduced from ref. [32] with permission of Academic Press.

$$\begin{aligned}
\mathcal{H} = & \sum_{i\sigma} [\epsilon_0 n_{i\sigma} + g\mu_B H_i \text{sign}(\sigma)] + \sum_{\langle ij \rangle} t_{ij} [c_{i\sigma}^+ c_{j\sigma} + h.c.] + \sum_i U_i n_{i\uparrow} n_{i\downarrow} \\
& + \sum_{\langle ij \rangle \alpha\beta} J_{ij} c_{i\alpha}^+ c_{i\beta} c_{j\beta}^+ c_{j\alpha} + H_z \sum_{i\sigma} g\mu_B n_{i\sigma} \text{sign}(\sigma)
\end{aligned} \tag{30}$$

where the first term denotes the electron energy in the i th dot, (H_i is a z-directed magnetic field applied selectively to the i th dot with, say, a spin polarized scanning tunneling microscope (SPSTM) tip, to orient its spin polarization), the second term denotes the hopping between the dots, the third term is the Coulomb repulsion within the i th dot, the fourth term is the exchange interaction between nearest neighbor dots, and the last term is the Zeeman splitting induced by the globally applied magnetic field H_z directed along the z-direction.

Molotkov and Nazin [39] have simplified this Hamiltonian to the Heisenberg model which yields

$$\mathcal{H} = J \sum_{\langle ij \rangle} \sigma_{zi} \sigma_{zj} + J \sum_{\langle ij \rangle} [\sigma_{xi} \sigma_{xj} + \sigma_{yi} \sigma_{yj}] + \sum_{\text{input dots}} \sigma_{zi} h_{zi}^{\text{input}} \quad (J > 0) \tag{31}$$

where we have neglected the global magnetic field H_z . The quantity J is the exchange splitting and h_{zi}^{input} is the Zeeman splitting caused by the local magnetic field applied with, say an SPSTM tip, to the i th dot to orient the spin(s) of its electron(s).

The above Hamiltonians describe any number of dots, each containing any number of electrons. Here, we are concerned with the special case of just two dots each containing only one electron. We will call these two dots A and B , where A is the input dot (whose spin polarization is set by an external SPSTM tip to conform to the input bit) and B is the output dot. Let us consider the case when the input bit corresponds to “upspin”.

In the basis of two electron states, the Hamiltonian in Equation (2) can be written as

$$\begin{array}{cccc}
& |\downarrow\downarrow\rangle & |\downarrow\uparrow\rangle & |\uparrow\downarrow\rangle & |\uparrow\uparrow\rangle \\
\left(\begin{array}{cccc}
h_A + J & 0 & 0 & 0 \\
0 & h_A - J & 2J & 0 \\
0 & 2J & -h_A - J & 0 \\
0 & 0 & 0 & -h_A + J
\end{array} \right) & \begin{array}{l} |\downarrow\downarrow\rangle \\ |\downarrow\uparrow\rangle \\ |\uparrow\downarrow\rangle \\ |\uparrow\uparrow\rangle \end{array} & & \tag{32}
\end{array}$$

where h_A is the Zeeman splitting caused by the externally applied local magnetic field in input dot A.

The eigenenergies and eigenstates of the above Hamiltonian are found by diagonalizing

Eigenenergies	Eigenstates
$h_A + J$	$ \downarrow\downarrow\rangle$
$-J + \sqrt{h_A^2 + 4J^2}$	$\sqrt{\frac{1}{2} \left(1 + \frac{h_A}{\sqrt{h_A^2 + 4J^2}}\right)} \uparrow\downarrow\rangle + \sqrt{\frac{1}{2} \left(1 - \frac{h_A}{\sqrt{h_A^2 + 4J^2}}\right)} \downarrow\uparrow\rangle$
$-J - \sqrt{h_A^2 + 4J^2}$	$\sqrt{\frac{1}{2} \left(1 - \frac{h_A}{\sqrt{h_A^2 + 4J^2}}\right)} \uparrow\downarrow\rangle - \sqrt{\frac{1}{2} \left(1 + \frac{h_A}{\sqrt{h_A^2 + 4J^2}}\right)} \downarrow\uparrow\rangle$
$-h_A + J$	$ \uparrow\uparrow\rangle$

In the absence of any applied local magnetic field ($h_A = 0$), the ground state energy is $-3J$ and the ground state wave function is $\frac{1}{\sqrt{2}}(|\uparrow\downarrow\rangle - |\downarrow\uparrow\rangle)$ which is an entangled state in that neither the input dot nor the output dot has a definite spin polarization.

In ref. [32], we showed that if the system is initially in the ground state and a local magnetic field is applied to the input dot A at time $t=0$ to align its spin polarization to the “up” state, then unitary evolution of the system according to

$$\psi(t) = \exp[-i\mathcal{H}t/\hbar]\psi(0), \quad (33)$$

mandates that the wave function at time t , is given by

$$\psi(t) = c_2(t)|\uparrow\downarrow\rangle + c_3(t)|\downarrow\uparrow\rangle \quad (34)$$

where

$$\begin{aligned} c_2(t) &= \frac{e^{iJt/\hbar}}{\sqrt{2}} \left[\cos(\omega t) - i \left(\frac{h_A}{\hbar\omega} + \sqrt{1 - \frac{h_A^2}{\hbar^2\omega^2}} \right) \sin(\omega t) \right] \\ c_3(t) &= -\frac{e^{iJt/\hbar}}{\sqrt{2}} \left[\cos(\omega t) - i \left(\frac{h_A}{\hbar\omega} - \sqrt{1 - \frac{h_A^2}{\hbar^2\omega^2}} \right) \sin(\omega t) \right] \end{aligned} \quad (35)$$

and $\hbar\omega = \sqrt{h_A^2 + 4J^2}$

If the system were to act as an inverter, it should ultimately reach the state $|\uparrow\downarrow\rangle$. This desired state however is not an eigenstate of the system. Consequently, the system will continue to evolve to a different state unless a “read” operation collapses the wave function as soon as the desired state is reached. The time to reach the desired state, which we will designate the switching time, is given by

$$\tau_d = \frac{h}{4\sqrt{h_A^2 + 4J^2}} \quad (36)$$

Note that this time must be much shorter than \hbar/kT in order to maintain reasonable coherence in quantum computing [40]. This can be achieved by making $J \gg kT$. For 100 Å diameter dots separated by 1 eV high and 20 Å wide barriers, the exchange splitting J can be on the order of 100 meV in semiconductors.

If the inverter's initial state is the ground state, then it is possible to switch the inverter *completely* (i.e. $c_2(\tau_d) = 1, c_1(\tau_d) = c_3(\tau_d) = c_4(\tau_d) = 0$) if $h_A = 2J$. However, if the initial state is not the ground state, then the inverter can never switch completely to the desired state, (i.e. $c_2(\tau_d) < 1$). Nonetheless, we can still define a switching time as the delay that elapses before the closest approach to the desired state (in other words the time required to reach the maximum value of c_2). This switching time is still given by Equation (6). This equation also shows that the inverter will “switch” in a finite time *even if* the switching energy $h_A \rightarrow 0$. However, the “switching” is ephemeral since the system will continue to evolve unitarily unless a read operation collapses the wave function at the right juncture.

In this system, there is no dissipation whatsoever except during the read operation. Therefore, the product of dissipated energy and switching delay (necessary to complete the computation) can obviously be zero. The product of applied energy and switching delay is

$$h_A \tau_d = \frac{\hbar h_A}{4\sqrt{h_A^2 + 4J^2}} \quad (37)$$

We immediately see that any energy-time uncertainty that might have been expected is violated

$$h_A \tau_d < \frac{\hbar}{2} \quad \text{if } h_A < \frac{2J}{\sqrt{\pi^2 - 1}} \quad (38)$$

Thus we can violate the uncertainty by making h_A arbitrarily small (and yet switching in a finite time). It should be emphasized that h_A is the energy applied to switch the inverter and is not necessarily *dissipated*. Even if it were completely dissipated, the above equation would still clearly show that there is no energy-time uncertainty limitation on (dissipated) energy-delay product, contrary to the popular view espoused in [41, 42]. Landauer agrees that there is no limit imposed by the uncertainty principle as per as dissipated energy is concerned [43]. In fact, concrete and detailed classical models of dissipationless computation have been provided by several authors and numerous quantum mechanical models of dissipationless computation have also been forwarded starting with the early work of Benioff [6, 44]. These models require no dissipated energy, but usually do require input energy to switch. What we see in the pathological example above is that

there is no energy-time uncertainty limit even when the energy concerned is the *applied energy* rather than the dissipated energy. Computation can proceed by applying arbitrarily small energy to initiate the process.

10 Coulomb Coupled Quantum Dots for Toffoli-Fredkin Gate and Quantum Computation

In the previous section, we described a quantum inverter. An inverter however is not a universal gate. The Toffoli-Fredkin gate is a mathematically (and hence physically) reversible three-bit *universal* gate with three inputs A, B, C and three outputs A', B' and C' .

As mentioned before, in this gate, $A' = A$ and $B' = B$. The bit $C' = \bar{C}$ only if $A = B = 1$. Otherwise, $C' = C$.

A physical realization of the Toffoli-Fredkin gate that is most easily amenable to nanoelectronic adaptations was proposed by Seth Lloyd [25] expanding on ideas set forth earlier by Mahler, et. al. [45]. The Lloyd architecture consists of an array of three weakly coupled quantum systems A, B and C . Each system can exist in one of two energy states E_0^i and E_1^i ($i \in A, B, C$) which represent logic 0 and 1. Furthermore, A, B, C are distinct systems such that the resonant energies $\hbar\omega_i = E_1^i - E_0^i$ are different for each of them ($\omega_A \neq \omega_B \neq \omega_C$). A π_i pulse is a radiation that obeys the condition

$$\frac{1}{\hbar} \int \vec{\mu}_B^i \cdot \hat{e} \mathcal{E}(t) dt = \pi \quad (39)$$

where $\vec{\mu}_B^i$ is the induced dipole moment between the ground state and excited state of the i -th system, \hat{e} is the polarization unit vector of the incident radiation and $\mathcal{E}(t)$ is the magnitude of the pulse envelope at time t . Such a pulse flips the i -th system from the excited state to the ground state and vice-versa. It is assumed that the duration of this pulse is much shorter than the inverse of the spontaneous decay rate from the excited to the ground state.

Because of the nearest-neighbor interaction between A, B and C , the resonant energies $\hbar\omega_i$ for each of them is no longer unique and depends on whether its nearest neighbors are in the excited or ground state. Thus

$$\omega_A \rightarrow \omega_0^A, \omega_1^A$$

$$\begin{aligned}
\omega_B &\rightarrow \omega_{00}^B, \omega_{01}^B, \omega_{10}^B, \omega_{11}^B \\
\omega_C &\rightarrow \omega_0^C, \omega_1^C
\end{aligned}
\tag{40}$$

Here, the subscripts on the right hand side refer to the states of the corresponding system's nearest neighbor(s). For instance, ω_{00}^B is the resonant frequency of system B when its two neighbors A and C are both in their ground states.

A Toffoli gate can be realized by shining a π pulse with frequency ω_{11}^B . The state of B is inverted only if both A and C are in their excited states. This characteristic realizes the truth table of a Toffoli gate.

10.1 Connecting Toffoli-Fredkin gates

In order to do computation, one needs to connect various Toffoli gates. This can be realized without physical wires if we have a linear array consisting of units ABC, ABC, \dots . Computation is performed by first initializing the array to the input with appropriate sequence of π pulses and then applying another series of π pulses to complete the computation. This methodology was described in detail in Ref. [25].

The above system can also be used to perform quantum computation if both π and $\pi/2$ pulses are used. A $\pi_i/2$ pulse puts the i -th system in a state $1/\sqrt{2}(|1\rangle - |0\rangle)$ which is a “qubit” in the coherent superposition of bits 1 and 2. By using an appropriate pulse train, one can perform quantum computation.

Rolf Landauer, an ardent critic and astute examiner of all “quantum schemes”, has criticized this implementation from two angles. First, this gate is not truly dissipationless unless the π or $\pi/2$ pulses can be recycled. This would also require that they are not distorted by interaction with the system. Second, interaction with the environment will cause errors and error correction will require dissipation. In principle, the latter objection is no longer serious in view of the recent advances in quantum error control coding [50, 52, 51]. Errors can be corrected by “software” rather than “hardware” countermeasures. Of course, this is done at the expense of increased memory and a larger system may decohere more quickly than a smaller system. Therefore, error correction comes with a cost, just as everything else does.

Landauer's first criticism is much more difficult to rebut. Photon recycling is not an unheard of concept in solid state systems [46, 47, 48, 49] but it is difficult. The requirement that the pulse

shape remain undistorted in any wave guide is a tall order. This would require the wave guide to have specific non-linearities so that the pulses essentially become solitons. At this time, one does not have a suitable design for such a recycler.

We will next examine a specific implementation of Lloyd’s generic ideas and provide a concrete example of a Toffoli-Fredkin gate. This example is suitable for nanoelectronics and is due to Alexander Balandin and the author.

10.2 Nanoelectronic version of a Toffoli-Fredkin gate

Consider an array of three quantum dots with high barriers (Fig. 3). Each houses a single conduction band electron.

For high enough barriers, we can neglect any overlap between the wave functions of electrons in adjacent dots, and write the many-body wave function of the three-electron system as a product of three single particle wave functions in the Hartree approximation

$$\Psi_{n,k,l} \equiv \Psi_{n,k,l}(x_1, x_2, x_3) = \psi_n(x_1)\phi_k(x_2)\chi_l(x_3), \quad (41)$$

where $\psi_n(x_1)$, $\phi_k(x_2)$, and $\chi_l(x_3)$ are the single electron envelope functions for the first, second and third dots, respectively. Subscripts n , k , l denote conduction subband levels. We assume that each dot has two bound states in the conduction band so that each electron can occupy either ground state ($n=1$, $k=1$, or $l=1$) or the excited state ($n=2$, $k=2$, or $l=2$). These two states encode logic bits 1 and 0.

Owing to Coulomb interaction, the resonant frequency for transitions between the excited and ground states in one dot depends on whether the electron(s) in the neighboring dot(s) are in the excited or ground state. For the central dot, this means that $\omega_{11} \neq \omega_{10} \neq \omega_{01} \neq \omega_{00}$. This forms the basis of a Toffoli-Fredkin gate. Note that in reality, a single gate only requires that ω_{11} be distinct. However, arbitrary data manipulation requires that all ω ’s be distinct.

Let us calculate the resonant transition frequency of the central quantum well as a function of two adjacent wells’ states. We denote the widths of the well as d , a , and b (see Fig. 3) and will refer to them as the “left” well (L), the “central” well (C), and the “right” well (R), respectively. The barrier thicknesses are W and H . The first order perturbation corrections to the energy of the k subband of the C well are given by the expression

$$E_{n,k,l} = E_k + \langle \Psi_{n,k,l} | V(x_3 - x_2) | \Psi_{n,k,l} \rangle + \langle \Psi_{n,k,l} | V(x_1 - x_2) | \Psi_{n,k,l} \rangle, \quad (42)$$

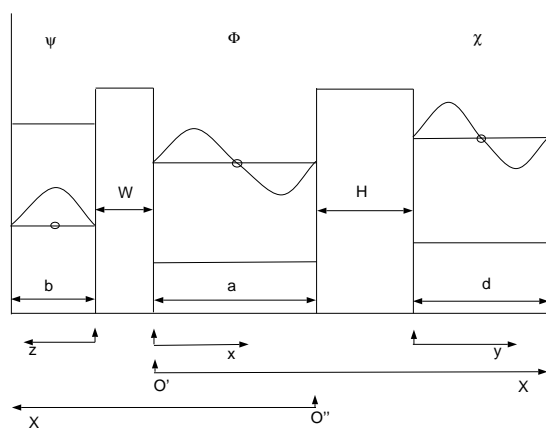


Figure 3: The potential profile for a three-dot system showing the wave function envelopes for the ground and excited states. Reproduced from ref. [33] with permission of Academic Press.

where $V(x_i - x_j)$ is the Coulomb interaction terms, x_i are absolute coordinates of electrons belonging to different wells, m^* is the effective mass of the conduction band electron, E_k is the unperturbed confined energy which is given for the square well potential by a regular expression

$$E_k = \frac{k^2 \pi^2 \hbar^2}{2m^* a^2}. \quad (43)$$

To simplify the calculation, we define a set of local coordinate systems (see Fig. 3). Substituting in Eq. 41, the electron envelope functions for the square well potential (written in local coordinates), can be rewritten as

$$\Psi_{n,k,l} = \sqrt{\frac{2}{d}} \sin\left(\frac{\pi n z}{d}\right) \sqrt{\frac{2}{a}} \sin\left(\frac{\pi k x}{a}\right) \sqrt{\frac{2}{b}} \sin\left(\frac{\pi l y}{b}\right). \quad (44)$$

The distance between electrons in the R and C wells (in O' coordinate system) is $x_3 - x_2 = a + W + y - x$, while the distance between electrons in the L and C wells (in O'' coordinate system) is $x_1 - x_2 = a + H + z - x$. With the limits of integrations determined by the well boundaries, Eq. 42 now reads

$$E_{n,k,l} = \frac{\pi^2 \hbar^2 k^2}{2m^* a^2} + \frac{e^2}{\pi \epsilon^* a b} \int_{x=0}^a \int_{y=0}^b \frac{\sin^2(\pi k x/a) \sin^2(\pi l y/b)}{a + W + y - x} dx dy \quad (45)$$

$$+ \frac{e^2}{\pi \epsilon^* a d} \int_{x=0}^a \int_{z=0}^d \frac{\sin^2(\pi k x/a) \sin^2(\pi n z/d)}{a + H + z - x} dx dz,$$

where $\epsilon^* = f_b \epsilon_b + f_w \epsilon_w$ is an effective dielectric constant of the system, f_b (f_w) and ϵ_b (ϵ_w) are the volume fraction and dielectric constant of the barrier (well) material, respectively. Note that with this definition ϵ^* is a function of well width when the barrier thickness is fixed.

The energy of the transition between the first excited state ($k = 2$) and the ground state ($k = 1$) in the central well can now be written as a function of the principal numbers n and l of the neighboring wells:

$$\Delta E_{n,l} = \frac{3\pi^2 \hbar^2}{2m^* a^2} + \frac{e^2}{\pi \epsilon^* a b} \int_{x=0}^a \int_{y=0}^b \frac{\sin(3\pi x/a) \sin(\pi x/a) \sin^2(\pi l y/b)}{a + W + y - x} dx dy \quad (46)$$

$$+ \frac{e^2}{\pi \epsilon^* a d} \int_{x=0}^a \int_{z=0}^d \frac{\sin(3\pi k x/a) \sin(\pi k x/a) \sin^2(\pi n z/d)}{a + H + z - x} dx dz.$$

Here we have utilized some trigonometrical equalities to simplify the result of the subtraction $\Delta E_{n,l} = E_{n,2,l} - E_{n,1,l}$.

In order to be able to build a conditional quantum gate (or the Toffoli-Fredkin gate), the transition energy $\Delta E_{n,l}$ should be different for all possible quantum state $\{|n\rangle, |l\rangle\}$: $\Delta E_{1,2} \neq \Delta E_{2,1} \neq \Delta E_{1,1} \neq \Delta E_{2,2}$. Obviously, the two states which are most difficult to resolve are $\{|1\rangle$

, $|2 \rangle$ and $\{|2 \rangle, |1 \rangle\}$. For convenience, we write here explicitly the energy difference between these two states

$$\Delta E_{1,2} - \Delta E_{2,1} = \frac{e^2}{\pi\epsilon^*a} \int_{x=0}^a \left(\int_{y=0}^b \frac{\sin(3\pi x/a)\sin(\pi x/a)\sin(3\pi y/b)\sin(\pi y/b)}{b(a+W+y-x)} dy \right. \quad (47)$$

$$\left. \int_{z=d}^0 \frac{\sin(3\pi kx/a)\sin(\pi kx/a)\sin(\pi z/d)\sin(3\pi z/d)}{d(a+H+z-x)} dz \right) dx.$$

To derive the above equation, we used the fact that $\sin^2(2\pi y/b) - \sin^2(\pi y/b) = \sin(3\pi y/b)\sin(\pi y/b)$, and changed the limits of integration. For the special case when $W = H$, this equation can be further simplified by substitution of variable in the integrand to

$$\Delta E_{1,2} - \Delta E_{2,1} = \frac{e^2}{\pi\epsilon^*a} \int_{x=0}^a \int_{u=d}^b \frac{d\sin(3\pi u/b)\sin(\pi u/b) + b\sin(3\pi u/d)\sin(\pi u/d)}{bd(a+H+u-x)} \quad (48)$$

$$\times \sin(3\pi kx/a)\sin(\pi kx/a) du dx.$$

It is easy to see from the last equation that when the thicknesses of two peripheral wells and barriers are equal ($d = b$ and $W = H$), the states $\{|1 \rangle, |2 \rangle\}$ and $\{|2 \rangle, |1 \rangle\}$ are degenerate and can not be resolved. This is a direct result of the symmetry of the system and can be easily guessed without mathematical consideration. More interesting consequence of Equations 47 and 48 is that there exists a ratio of b/d ($\neq 1$) such that the integral in Equation 48 vanishes, and the states are degenerate again. The physical origin of this additional degeneracy will be discussed later. One should find optimum values of well thicknesses b and d such that the states $\{|1 \rangle, |2 \rangle\}$ and $\{|2 \rangle, |1 \rangle\}$ are resolved.

10.3 Resonant energies in Coulomb coupled dots

In calculating resonant energies in Coulomb coupled dots, we will concentrate mostly on two material systems. The first is *InAs* characterized by light electron effective mass $m^*(InAs) = 0.023m_o$ and strong dielectric screening $\epsilon(InAs) = 14.6$ (m_o is the free electron mass). The second is *CdS* which is characterized by heavy electron effective mass $m^*(CdS) = 0.21m_o$ and relatively weak dielectric screening $\epsilon(CdS) = 5.4$ for the frequencies close to band gap resonance and $\epsilon(CdS)$ approaching 3.1 for the infrared region relevant to intraband transitions.

In order to find optimum values of peripheral well thicknesses, we will calculate transition energy $\Delta E_{n,l}$ as a function of the R well thickness b while fixing the L well thickness d and using it as a parameter. For simplicity, the thickness of the left barrier will be assumed to be equal to that on

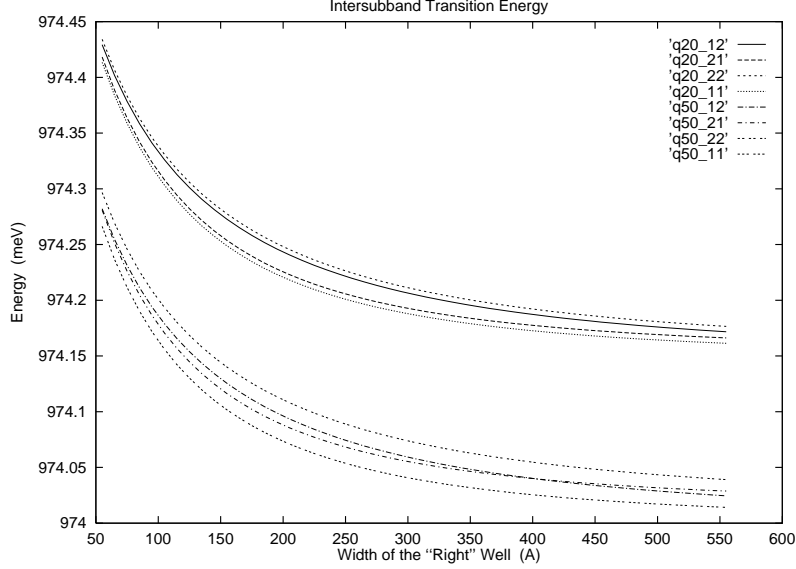


Figure 4: Energy of the transition between the first excited and ground states in the ‘‘central well’’ as a function of the width of the ‘‘right’’ well. The upper family of curves corresponds to the ‘‘left’’ well width of 20\AA , the lower one corresponds to the ‘‘left’’ well width of 50\AA . The results are shown for all four possible combination of states in the two extremal wells. Material parameters for InAs have been used. Reproduced from ref. [33] with permission of Academic Press.

the right ($W = H$). These thicknesses will be assumed to be 20\AA unless otherwise stated. This value of the barrier thickness guarantees negligible barrier penetration of the wave function.

In Fig. 4, we present the energy of the transition between the first excited state and the ground state in the C well as a function of the R well width (b). The curves are shown for *InAs* quantum wells. The thickness of the C well is 100\AA . The L well width is varied over two values: 20\AA and 50\AA . It is interesting to note that the splittings between worst-resolved states attain maximum values when b is in the range $150 - 170\text{\AA}$. Moreover, the states $\{|1\rangle, |2\rangle\}$ and $\{|2\rangle, |1\rangle\}$ are degenerate not only at $b = d = 50\text{\AA}$ but also at $b \approx 400\text{\AA}$. At first, this may appear surprising. The physical origin of the additional degeneracy lies in the fact that Coulomb perturbation to the transition energies depends on the distance between particles as well as on the electron envelopes which serve as weight functions in the integrand in Eq. 48. Consequently, at some values of $b/d \neq 1$ the integration over u in Eq. 48 vanishes.

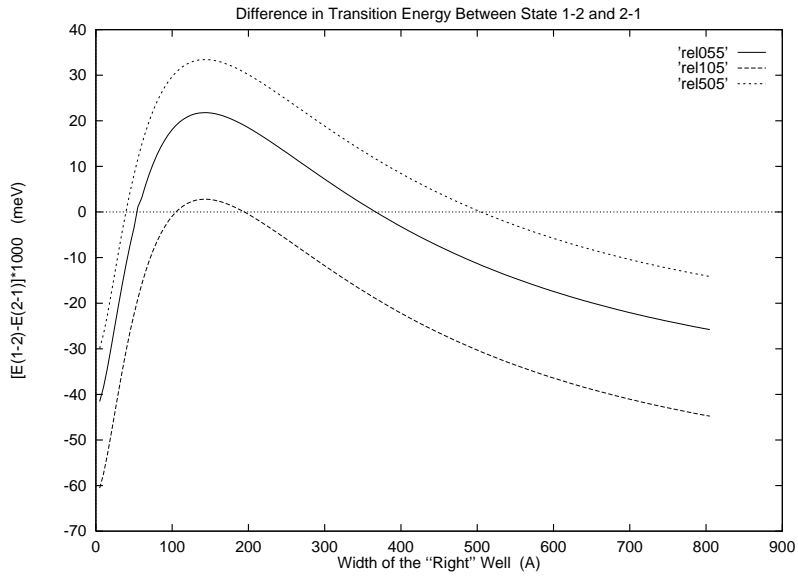


Figure 5: The difference in transition energy $\Delta E_{1,2} - \Delta E_{2,1}$ as a function of the width of the “right” well. The results are shown for three different values of the width of the “left” well. The material parameters used for calculation correspond to *InAs*. Reproduced from ref. [33] with permission of Academic Press.

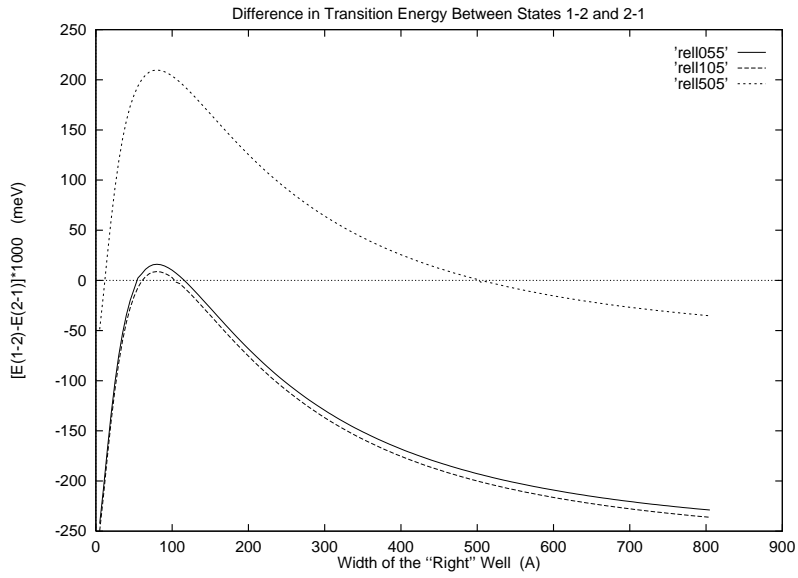


Figure 6: The difference in transition energy $\Delta E_{1,2} - \Delta E_{2,1}$ as a function of the width of the “right” well. The results are shown for three different values of the width of the “left” well. The material parameters used for this calculation correspond to *CdS*. Reproduced from ref. [33] with permission of Academic Press.

In order to examine the behavior of the worst resolved states $\{|1 \rangle, |2 \rangle\}$ and $\{|2 \rangle, |1 \rangle\}$, we plot separately the difference in transition energy between these two states as a function of the R well thickness (see Fig. 5). The L well thickness is chosen to be 55\AA (solid line), 105\AA (dashed line), and 505\AA (dotted line). As one can see, the average splitting is very small for this system and represents a fraction of meV at its maximum. Each curve has an additional degeneracy ($\Delta E_{1,2} - \Delta E_{2,1} = 0$) at $b/d \neq 1$ which should be avoided while designing the logic gate. Since $\Delta E_{1,2} - \Delta E_{2,1}$ does not depend on m^* (see Eq. 46) and strongly depends on ϵ^* , one can expect that the resolution of the $\{|1 \rangle, |2 \rangle\}$ and $\{|2 \rangle, |1 \rangle\}$ states will be better for *CdS* and any other system with lower dielectric constant. This is indeed the case, and it is clearly seen in Fig. 6. The splitting between states is an order of magnitude higher for the *CdS* system compared to the *InAs* system.

It is intuitively clear that in order to increase the energy difference between $\{|1 \rangle, |2 \rangle\}$ and $\{|2 \rangle, |1 \rangle\}$ states, one should introduce higher asymmetry into the system. Apart from varying the R well thickness, it is possible to break the symmetry by changing the barrier thickness. One can notice that increasing the width of one of the barriers decreases the energy separation between $\{|1 \rangle, |1 \rangle\}$ and $\{|2 \rangle, |2 \rangle\}$ states but increases it for $\{|1 \rangle, |2 \rangle\}$ and $\{|2 \rangle, |1 \rangle\}$ states. The degeneracies ($b = 50\text{\AA}$ and $b \approx 400\text{\AA}$), for the uniform barrier system, disappear for a system with different barriers. This is of course also desirable from architectural considerations. Another potential way of increasing the energy splitting between $\{|1 \rangle, |2 \rangle\}$ and $\{|2 \rangle, |1 \rangle\}$ states is through engineering the potential profile. One well can be rectangular and the other parabolic. This may be achieved through dopant grading.

11 A 2-qubit “spintronic” universal quantum gate

Today, most experimental effort in realizing semiconductor solid-state versions of universal 2-qubit gates is focused on the realization of a quantum controlled NOT or XOR gate. These are the two most popular gates. In these gates, one of the two qubits is called the target qubit and the other is the control qubit. The basic operation of the controlled NOT gate has two ingredients: (i) arbitrary rotation of the target qubit, and (ii) controlled rotation of the target qubit through specified angles if and only if the control qubit is in a certain state. The controlled XOR gate has similar dynamics: (i) arbitrary rotation of the target qubit, and (ii) a so-called “square-root-of-swap” operation where the

quantum states of the target and control qubits are half-way interchanged. More on this operation later.

There is now a consensus that in semiconductor solid state realizations, it is advantageous to encode the qubit in spin degrees of freedom of an electron or hole rather than charge degrees of freedom because of the much longer coherence times associated with spin. The charge coherence time saturates to about 1 nsec in most solids as the temperature is lowered to microkelvins. This is supposedly due to coupling of the electron to the zero-point motion of phonons (quantum noise) [57]. In contrast, the spin coherence time of an electron can be as long as a few milliseconds in materials such as silicon where the Landé g-factor is close to 2 (the free electron's g-factor) [58]. Nuclear spins can live even longer, perhaps an hour. Compound semiconductors may exhibit somewhat shorter electron spin coherence times, but spin coherence times as long as 100 ns have been experimentally demonstrated in n-type GaAs at the relatively balmy temperature of 5 K [65]. Consequently, there have been a number of “spintronic” proposals for quantum gates.

11.1 The Kane model

The first comprehensive solid state scalable realization of a universal 2-qubit spintronic quantum gate is due to Kane [59]. Qubits are encoded in the nuclear spin orientations of ^{31}P dopant atoms in silicon. These nuclear spins have very long coherence times, possibly several milliseconds at 4.2 K temperature. A particular target qubit (nuclear spin) is rotated by bringing the spin splitting energy of that nucleus in resonance with a global ac magnetic field for specific duration. The spin-splitting energy is altered (using the hyperfine interaction) by changing the wave function of the electron bound to the target nucleus. This is done by applying a potential to that electron via a lithographically defined gate (called an “A-gate”) placed precisely on top of that nucleus. The gate potential attracts or repels the electron thereby changing its wave function, and hence the nucleus' spin-splitting energy. The 2-qubit operation is achieved by yet another set of lithographically defined gates (called “J gates”) which raise or lower a potential barrier between two neighboring nuclei's electrons (one nucleus is the “target” and the other is the “control” qubit). As the barrier is lowered, the wave functions of the two adjacent electrons overlap and the resulting exchange interaction lowers the energy of the singlet state with respect to the triplet state (as long as there is no magnetic field to induce a Zeeman splitting that exceeds the exchange splitting). Thus, the rotation of the target qubit by the global ac magnetic field can be made conditional on the spin

state of the control qubit. This realizes the quantum controlled NOT operation.

A closely related proposal that hosts qubits in electronic spin, rather than nuclear spin, has been forwarded by Vrijen et. al. [60]. This model eliminates the need to transduce the qubit between nuclear and electron spin. The penalty is the Instead of using hyperfine interaction to change the spin splitting energy in a target qubit, they utilize a Si/SiGe heterostructure. The ^{31}P dopant atom has to be placed exactly at the interface of this two materials and a lithographically delineated gate has to be aligned exactly on top of this buried dopant atom. The lateral alignment may be achieved by ion-implanting the dopant through a mask [61], but the vertical alignment is much more difficult. One has to virtually eliminate “straggle” in ion implantation. This is a very tall order.

An additional complication in these models is the read/write mechanism for qubits. Reading is performed by “measuring” the spin polarization electronically without the aid of anything analogous to a Stern-Gerlach apparatus. One suggested possibility is to use Pauli principle [60]. An electron is maintained in a quantum dot in given spin state. The electron to be probed is injected towards that quantum dot. If the two spins are anti-parallel, there is no Pauli blockade (in addition to the normal Coulomb blockade), and the target electron will enter the dot. Therefore, the dot’s charge will change and this can be monitored by single-electron electrometers. This is just the basic idea. Actual implementation may involve some refinements.

An earlier proposal, incorporating spintronics but without any mechanism for maneuvering qubits, was presented by Privman [62]. This will not be discussed at any length since it does not constitute a true quantum gate.

11.2 An alternate quantum dot based spintronic model

We have proposed an alternate model that is much easier to synthesize than the Kane model or its modification by Vrijen [63]. Particularly, the read/write scheme is vastly simpler since we propose using ferromagnetic contacts for spin injection and detection. The notion of using ferromagnetic contacts as spin polarizer and spin analyzer has been around for at least ten years [71]. I describe this paradigm below.

Consider a semiconductor quantum dot capped by two spin-polarized ferromagnetic layers (see Fig 7). Insulating layers are interposed between the semiconductor and ferromagnet to provide a confining potential for an electron in the semiconductor dot. A single spin-polarized quantum

(electron or hole) is injected into the semiconductor dot from a ferromagnetic contact, and trapped there by Coulomb blockade.

The ground state of the trapped quanton is automatically spin-split because of two effects: (i) the dc magnetic field caused by the ferromagnetic contacts introduces a Zeeman splitting, and (ii) the intrinsic electric field at the interface between the quantum dot and the surrounding material causes an additional spin splitting because of the Rashba (spin-orbit) interaction [67, 66, 71]. The total spin splitting is a combination of the Rashba and Zeeman splittings.

The Rashba component can be varied by an external gate potential [70]. Applying an electric field in the y - z plane using the contacts A_1, A_1' (see Fig. 7) modulates the energy splitting between the $+x$ -polarized (spin-up) and $-x$ -polarized (spin-down) states in the quantum dot. This controllability of the spin splitting energy with an external gate potential (because of the Rashba effect) is exploited to execute single qubit rotations (rotating the spin through arbitrary angles). The dependence of the total spin splitting energy in this structure on the gate potential is derived in the Appendix.

11.3 Single qubit rotations

To rotate the spin (single qubit) in a targeted quantum dot, we will modulate the Rashba component (and hence the total spin splitting energy) in that dot with a gate potential (applied through lithographically defined gates) to make it resonant with a *globally* applied ac magnetic field. This will induce transitions between the two spin states in that particular dot. Other dots remain unaffected. Depending on the amplitude of the magnetic field and duration of the interaction, the spin will rotate through chosen angles. The angle through which the spin rotates in a time T is given by

$$\theta = \frac{1}{\hbar} \int_0^T \vec{\mu}_B \cdot \vec{B} dt \quad (49)$$

We will apply a potential pulse of width T to the gate and this will rotate the spin through an angle θ . For instance, a π pulse ($\theta = \pi$) will flip the spin completely, whereas a $\pi/2$ pulse will place the quanton in an equal superposition of the two spin states if it was originally in one of the spin eigenstates. Thus, arbitrary qubit rotations in target dots can be achieved by controlling the width of the potential pulses applied at the gate and this realizes the first ingredient of a universal quantum gate, namely arbitrary single qubit rotations.

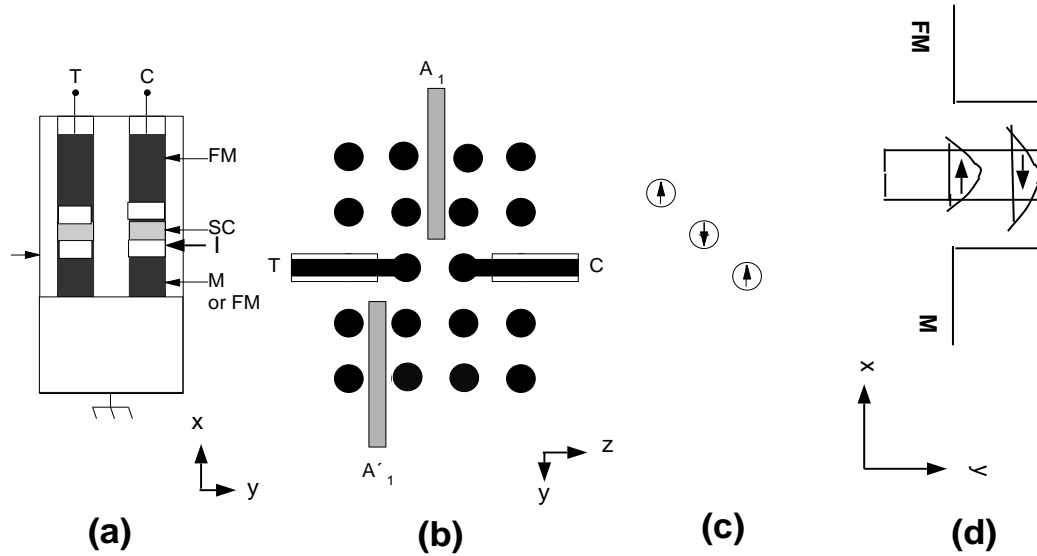


Figure 7: Schematic diagram showing the structure of a basic universal gate. a) Cross section of a single gate. FM, M, I and SC refer to ferromagnetic, metallic, insulating and semiconducting material respectively. C and T are ohmic contacts to the control and target qubit respectively. b) Top view of a gate within the dot array. Contacts labeled A are for applying electrostatic potentials to induce the Rashba effect, as well as turn on and off an exchange interaction between C and T. c) A ‘‘spin wire’’ for interconnecting gates. d) The conduction band diagram in the direction perpendicular to the heterostructures showing the spin-split levels. Spin splitting is caused by a combination of Zeemna effect and Rashba effect. For a ‘‘hole-qubit-structure’’ (See Fig..), the valence band diagram can be obtained by inverting this diagram. Reproduced from ref. [56] with permission from Elsevier Science.

11.4 Two qubit entanglement: Controlled dynamics of 2-qubit rotations

In order to achieve the second and last ingredient of a universal quantum gate – namely the conditional dynamics of a controlled NOT operation – we need to entangle 2 qubits and couple the rotation of one (target qubit) with the orientation of the other (control qubit). This can be done by turning on an exchange coupling between two single quantons in two neighboring dots for specified durations of time. If the coupling is turned on for a duration $h/2J$ (J is the exchange interaction energy), then the associated unitary time evolution corresponds to the “swap” operator which simply exchanges the quantum states of qubits 1 and 2. If the exchange is turned on for one-half of that duration, then the unitary evolution corresponds to a “square-root of swap”. By applying a sequence of unitary operations corresponding to single qubit rotations and the square-root of swap operation, one can realize the controlled NOT dynamics of a universal quantum gate [64].

The exchange coupling between the control (C) and target (T) dots can be varied by applying a positive potential (for electron qubits) or a negative potential (for hole qubits) to the contact A_1 which causes the electron- or hole-wave functions in C and T to leak out into the intervening barrier. This will turn the exchange coupling on. Thus, by applying appropriate potential pulses to various gates in the set (A_1, A_1') , we can realize the complete universal quantum gate.

11.5 Quantum connectors

An essential ingredient in quantum computers is “quantum connectors” that transmit quantum information, much in the same way as normal metal wires transmit voltages in a classical chip. A wire that transmits spin polarization is simply a linear array of exchange coupled single-electron quantum dots. The ground state of this array is anti-ferromagnetic so that the spin repeats itself in every other cell. Such as “spin wire” is shown in Fig. 7c.

11.6 Reading and writing of a qubit: spin polarizers and analyzers

“Writing” a qubit involves assigning a predetermined polarization to the spin. Thus, we need a spin polarizer for writing. We can inject the quanton with a fixed spin from the polarizer, and then rotate it by an appropriate angle to reach the desired initial orientation. The polarizer can be a spin-polarized ferromagnetic contact, or even an ordinary metal contact if the energy states in the

semiconductor dot are already spin split (see next section).

Reading a qubit involves measuring the spin orientation of the qubit. This is achieved in the same way as in a spin transistor [71]. A suitable potential is applied between the ferromagnetic contacts to make the quanton trapped in the semiconductor dot flow out into a ferromagnetic contact that acts as a spin analyzer. If the quanton's spin is oriented along the analyzer's magnetization, the analyzer transmits the quanton; else it reflects it. A transmitted quanton is therefore read as "spin-up", and the absence of a transmitted quanton is read as "spin-down". A qubit that has been read collapses to a classical binary bit with two possible values: "spin-up" and "spin-down". Single electron (or hole) currents or charge (due to a transmitted electron) can be detected by single electron electrometers that are exquisitely sensitive and can detect the charge of 10^{-8} electrons [79].

There are of course other strategies for reading a qubit, as mentioned before. It would cost more energy to inject a second quanton into a quantum dot if its spin is parallel to the one already occupying the dot (Pauli Exclusion Principle). The Pauli blockade will add to the Coulomb blockade in this case and hence, in principle, can be detected in tunneling current measurements. Methods using nanosized FETs have also been suggested for measuring single quanton spins [60], but is a lot more difficult than the present method. The problem with the Pauli blockade approach is that one must know the spin of the first quanton with certainty, in order to determine the spin of the second quanton. The spin of the first quanton can be fixed with a highly localized magnetic field that *must not affect* the spin of the second quanton. In principle, this can be done by generating a local magnetic field in a nanometer sized area that is magnetically shielded. This is extremely difficult. In contrast, our technique of reading spin using spin analyzers is much simpler.

12 Spin Coherence

We have proposed using the Rashba effect to select a target qubit for rotation. It is widely believed that this effect, which is an electric-field-induced spin orbit coupling, will degrade spin coherence and be detrimental to quantum computing. That is true for bulk, quantum wells and quantum wires, but *not* quantum dots. The use of quantum dots provides widespread immunity against spin decoherence.

There are three principal mechanisms of spin relaxation in a semiconductor: (i) the Elliott-Yafet mechanism, (ii) the D'yakonov-Perel mechanism, and (iii) the Bir-Aronov-Pikus mechanism [80].

The Elliott-Yafet mechanism [81] is based on the fact that in a real crystal, the Bloch states are not spin eigenstates. The spin orbit interaction mixes the spin-up and spin-down amplitudes. The Rashba effect *can* exacerbate this mixing. As a result of this mixing, ordinary scattering interactions with impurities, phonons, surfaces, etc., can flip spin. In a quantum dot however, the electron is completely stationary since the wavefunction is fully *real* and hence the expected value of the momentum in any direction is exactly zero. Since the electron does not move, it cannot suffer elastic collisions which changes the electron's momentum (since it cannot change energy). The only problem is therefore inelastic scattering (phonons). The Overhauser effect [82] is known to flip spin via phonon modulated scattering. Thus, phonons could be a nuisance.

In the context of quantum computing however, phonons are almost never a serious issue since the ambient temperature is usually very low (typically 300 mK - 4.2 K). Moreover, in a quantum dot, the phonon bottleneck effect mitigates phonon scattering to a large extent [83]. Thus, the Elliott-Yafet mechanism is very weak. A far more important decohering mechanism is electromagnetic interference from the gate. This is unavoidable in any gate controlled scheme. Again, the quantum dot helps in countering electromagnetic decoherence since it usually needs a phonon or infrared photon to carry away the dissipative energy. Because of the extremely restrictive selection rules for photon or phonon transitions in a quantum dot, the electromagnetic decoherence may be suppressed as well.

Another common spin decoherence mechanism (which dominates in semiconductor quantum wells or quantum wires where multiple subbands are occupied) is the D'yakonov-Perel mechanism [86]. An electron's spin precesses about the direction of its momentum, as long as the crystal lacks inversion symmetry and/or has a structural inversion asymmetry (such as due to a built-in electric field caused by doping gradients, compositional modulation, or an externally applied electric field). The crystal inversion asymmetry gives rise to Dresselhaus spin orbit interaction [84] and the structural inversion asymmetry gives rise to Rashba spin orbit interaction [67]. These spin orbit interactions are momentum dependent. They cause the spin to precess about an axis determined by the direction of the momentum. If the momentum changes randomly because of scattering, then the spin orientation changes randomly. When ensemble averaged over a large number of electrons, the ensemble average spin dephases [85]. This dephasing mechanism is the so-called D'yakonov-Perel' mechanism. In a quantum dot, there is no "momentum", and there is no "ensemble" of electrons either (we are talking of a single electron encoding the qubit). Therefore, the Dyakonov-Perel

mechanism does not exist.

What could be the most serious source of decoherence in a quantum dot is interactions with nuclear spins [87]. Therefore, one should choose the right material for the quantum dot; it should be isotopically pure and the nuclear spin will be small.

The last mechanism of concern is the Bir-Aronov-Pikus mechanism [88] which is based on electron-hole interaction. Since we are dealing with a single conduction band electron, injected from the contact into a depleted semiconductor, this mechanism is extremely weak.

In conclusion, the quantum dot is very forgiving in terms of spin coherence.

In the context of a quantum “computer” where several qubits are entangled (and therefore interact), there may be more subtle decoherence issues associated with many body effects. Dealing with decoherence in the interacting electron picture is rather challenging, and so far only few theoretical attempts have been made in that direction [89].

13 Coherent spin injection from spin polarized contacts

We mentioned earlier that we wish to inject an electron into the quantum dot with a definite spin orientation so that we know the initial state of the qubit at time $t = 0$. However, coherent spin injection from a spin-polarized (ferromagnetic) contact into the semiconductor is *not* critical for this purpose. If the spin-injection does not work, one could still select a definite initial spin using the principle of the spin-RTD. Since the subbands in the quantum dot are spin split, one can align the Fermi level in the contact with one of the spin-split levels and therefore preferentially inject into that level. This will assign a definite spin orientation to the qubit. If even that does not work, one can inject an electron with arbitrary spin and wait till the electron decays to the lowest state (by a spin flip transition if necessary). Since the spin degeneracy is lifted by a combination of the Zeeman and Rashba effect (see Appendix), the ground state always has a definite spin polarization. In the latter two scenarios, ferromagnetic contacts are not necessary.

Even though coherent spin “injection” is not critical, coherent spin “detection” is absolutely critical since it provides the mechanism for reading a qubit. The injector is a spin-polarizer and the detector is a spin-analyzer. We can do away with the polarizer, but not the analyzer. Thus, coherent spin injection across one of the ferromagnetic interfaces is necessary. If the analyzer does not work either, we have to rely on the mechanisms proposed in ref. [60] for reading spin which

are much more complicated.

Coherent spin injection from a metal into a semiconductor is a difficult problem [90] and has been recently addressed theoretically [72, 73]. It has been realized that efficient spin injection from a metallic ferromagnet into a semiconductor requires interposing a tunnel barrier of some sort (e.g. a Schottky barrier) between the two. There have been some scattered reports of spin injection from a metallic ferromagnet into a semiconductor [74, 75] and between two semiconductors of widely different bandgaps [76]. Recently, spin polarized hole injection was demonstrated from GaMnAs into GaAs [91] at around a temperature of 120 K. Prior to that, spin polarized injection from CdMnTe into CdTe was demonstrated [78], but the disadvantage in that case is that CdMnTe is not a permanent ferromagnet; the spin polarization needs to be maintained by a globally applied dc magnetic field which introduces a Zeeman splitting in CdMnTe. However, only a very small field is required since the effective Landé g-factor for electrons in dilute magnetic semiconductors is huge (~ 100). On the other hand, the advantage of CdMnTe is that it is lattice matched to CdTe and hence interface scattering is less of a problem. Most recently, 90% spin polarized electron injection was demonstrated from the dilute magnetic semiconductor $\text{Be}_x\text{Mn}_y\text{Zn}_{1-x-y}\text{Se}$ into GaAs at a temperature below 5 K [92] and at a relatively large magnetic field which induces a Zeeman splitting in the magnetic semiconductor. While the temperature is high enough for quantum computing applications, the applied magnetic field is too large and may flip the spin in the semiconductor quantum dot, thus corrupting the qubit. The problem of coherent spin injection from a ferromagnetic material into a semiconductor is a topic of much current research. It has a long history and rapid strides are being made in this field.

Another important question is how easy will it be to maintain single electron occupancy in each dot. As long as the energy cost to add an additional electron ($= e^2/2C$; C is the capacitance of the dot) significantly exceeds the thermal energy kT , only a single electron will occupy each dot. Uniform electron occupancy in arrays of $> 10^8$ dots has been shown experimentally [77].

13.1 Spin measurement

After quantum computation is over, we need to read the result by measuring the qubits. During this process, the qubits will collapse to classical bits. These classical bits are the measured spin orientations in relevant dots. They are measured by measuring the current that results when the potential over the dot is raised over the Coulomb blockade threshold. If we assume that

the differential phase-shift suffered by the spin in traversing the dot is negligible; in other words, transport through the dot does not rotate the spin, then the magnitude of the measured current can tell us the spin orientation [71]. It was shown in ref. [71] that the spin-polarized contacts act as electronic analogs of optical polarizers and analyzers, so the current will depend on the projection of the spin of the quantum dot's resident electron on the spin orientation in the contacts. Thus, by measuring the current, we can tell the spin orientation in any quantum dot.

13.2 Calibration

For each target dot, the gate potential V_{target} that needs to be applied to bring the spin-splitting energy in resonance with B_{ac} , can be calibrated following the procedure outlined by Kane [59]. With $B_{ac} = 0$, we measure the spin in a quantum dot. Then we switch on B_{ac} and sweep V over a range. Next B_{ac} is switched off and the spin is measured. The range of V is progressively increased till we find that the spin has flipped. We then proceed to narrow the range with successive iteration while making sure that the spin does flip in each iteration. Finally this allows us to ascertain V with an arbitrary degree of accuracy. As pointed out by Kane [59], the calibration procedure can, in principle, be carried out in parallel over several dots simultaneously and the voltages stored in adjacent capacitors. External circuitry will thus be needed only to control the timing of the biases (application of V_{target}) and not their magnitudes. While this is definitely an advantage, fabricating nanoscale capacitors adjacent to each individual dot is certainly not easy. Moreover, capacitors discharge over time, requiring frequent recalibration through refresh cycles; therefore, this may not be a significant advantage.

13.3 Input and Output Operations

Any computer is of course useless unless we are able to input and output data successfully. Since we are using spin-polarized contacts to inject an electron in each dot, we know the initial orientation. Those dots where the initial orientation is the one we want are left unperturbed while the spins in the remaining dots are flipped by resonating with B_{ac} . This process prepares the quantum computer in the initial state for a computation and can be viewed as the act of “writing” the input data. Computation then proceeds on this initial state by carrying out a desired sequence of controlled rotation operations. Reading the data is achieved as described before.

14 Experimental realization of a quantum gate

A team of researchers from the author’s group and the US Naval Research Laboratory have proposed three different structures grown by molecular beam epitaxy that are viable prototypes for a quantum gate. They are shown in Fig. 8.

The first two structures are for hole qubits and the last for an electron qubit. Each structure has at least one ferromagnetic layer that acts as a spin analyzer. A variant of the first structure was used in the past to demonstrate spin coherent injection of *holes* from GaMnAs (a ferromagnet below 120 K) into GaAs [91]. In these structures, GaMnAs is used as a “spin analyzer”, rather than a “spin polarizer”, since the spin analyzer is more critical.

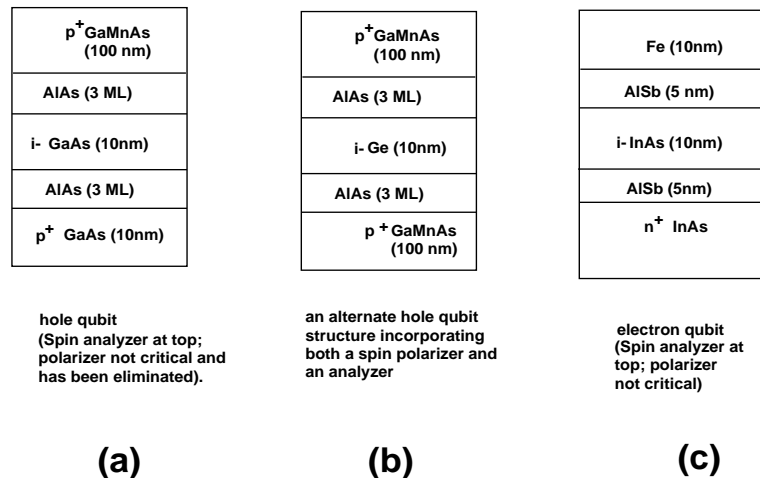


Figure 8: MBE-grown multilayered films for qubits: (a) a “hole-qubit” structure in which the GaMnAs ferromagnetic layer in the spin analyzer. The host for the qubit (a single hole) is the GaAs layer. This structure is the easiest to grow and has been demonstrated by Jonker, (b) an improved “hole-qubit” structure consisting of a GaMnAs polarizer and analyzer layer. The host of the qubit is Ge which has a smaller hole effective mass than GaAs and hence a stronger Rashba coupling for holes, (c) an “electron qubit” structure with Fe as the spin analyzer layer.

The hole qubit structure shown in Fig. 8(b) uses Ge as the semiconductor host for the qubit because Ge has a smaller hole effective mass than GaAs. The Rashba spin splitting energy is

inversely proportional to the effective mass of the quanton which motivates the choice of Ge. The use of Ge as opposed to GaAs has other advantages. The larger valence band offsets result in stronger hole confinement. Moreover, the hole spin coherence time in Ge, an elemental semiconductor, is probably *much longer* than in GaAs. Ge is essentially lattice matched to GaAs and high quality epilayers have been grown. Since Ge can be grown at low temperatures (compatible with GaMnAs), this structure can have two ferromagnetic layers: one at the top and one at the bottom. *Thus, it has both a spin polarizer and an analyzer.*

A structure for “electron-qubit” is shown in Fig. 8(c). It consists of an InAs quantum well to act as the host for the qubit, thin AlSb barriers, topped by a layer of Fe which serves as the spin analyzer. InAs is chosen because it has a large Landé g-factor which causes a larger Zeeman splitting (and hence indirectly a larger Rashba splitting (see Appendix)). It also has a small electron effective mass which directly enhances the Rashba splitting. It is the ideal material to host an electron qubit.

14.1 Creation of buried quantum dots using shallow etching and surface depletion

The semiconductor quantum dots must be *buried* dots as opposed to exposed dots for two reasons: (i) first, the interfaces of buried dots (which are defined by electrostatic depletion) are far superior to those of exposed dots, (ii) second, and more importantly, we need the wave functions of two neighboring dots to leak out into the intervening barrier and exchange-couple under the influence of a gate potential. This is needed in order to implement the “square-root of swap” operation which is necessary for the universal controlled-NOT gate. The barriers must be somewhat transparent for significant exchange coupling. These requirements are more easily met with “buried” dots. Buried dots can be created by shallow etching (sputtering) using etch masks that are delineated by either x-ray lithography (using resists) or by self-assembly (resistless). A side view of the finished quantum gate is shown in Fig. 9.

15 Quantum cryptography

We now venture into a very different field, quite distinct from quantum computing, namely “quantum cryptography”. Cryptography is the science of encoding confidential data in cryptic messages

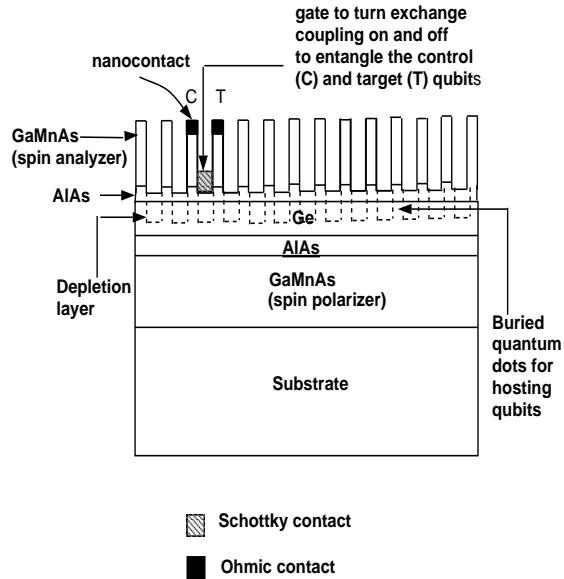


Figure 9: Shallow etched pillars defined on MBE grown films for creating buried quantum dots that host qubits. Reproduced with permission of Vasov Publishers from ref. [54].

and sending it over public channels to an intended receiver. An eavesdropper, who may intercept the message, should not be able to decipher it. Deciphering is accomplished via a “key” provided by the sender to the receiver alone. Nobody else should have this private key. In conventional classical cryptography, a “public key” is transmitted over a public channel and the actual “private key” is extracted from the public key by solving a trapdoor function such as factorizing a large number into its prime constituents. Although, solving the trapdoor function is difficult, it is theoretically *not impossible*. Worse still, if the eavesdropper succeeds in extracting the private key, neither the sender, nor the receiver will be aware of this. From then on, all secret transmissions will be compromised.

In the quantum world, there is no way to prevent an eavesdropper from intercepting the message, but once the eavesdropper does so, both the sender and receiver will become aware of her presence. Therefore, the intercepted key will be discarded and a new key will be sent out. The process will continue until an unintercepted key arrives at the receiver. The difference between quantum and classical cryptography is that in quantum cryptography, the eavesdropper can never remain hidden. Thus quantum cryptography is invariably more secure and unlike in the classical case, the final key

is *guaranteed* to be secure.

Charles Bennett and Gilles Brassard devised a quantum cryptography scheme based on the quantum no-cloning theorem and the impossibility of measuring certain pairs of observables simultaneously [93, 94]. The latter is the Heisenberg uncertainty principle which states that pairs of observables whose operators do not commute, cannot be measured simultaneously. The best known example of such pairs is the position and momentum of a quantum object (e.g. an electron). We will call such pairs “conjugate variables”. The no-cloning theorem is an extension of quantum measurement theory. In order to clone a quantum object, the cloning device must first measure it or examine it. In measuring one attribute of a quantum object (an observable), its conjugate pair partner is invariably disturbed, and disturbed unpredictably. Therefore, there is no way to capture a quantum object with complete fidelity which is a pre-requisite for cloning.

15.1 A quantum cryptosystem employing photons

Consider a photon which can be polarized in the so-called rectilinear basis, or the diagonal basis. The rectilinear basis corresponds to the photon’s electric field being aligned at 0° or 90° to some reference line on a plane, while the diagonal basis corresponds the electric field being aligned at 45° or 135° to the line. The rectilinear and diagonal polarizations are conjugate pairs and hence it is impossible to measure both of them exactly, at the same time.

In the humane convention of communication and information sciences, the sender A is always named Alice and the receiver B is always named Bob. Alice encodes the bits that she wants to send to Bob in a photon’s polarization by choosing either the rectilinear basis or the diagonal basis *randomly*. Her resulting polarization angle for each bit depends on the bit value and the chosen basis as follows:

Bit value	Chosen basis	Polarization angle
0	rectilinear	0°
1	rectilinear	90°
0	diagonal	45°
1	diagonal	135°

When Bob receives the bits, he measures them also in either the rectilinear or the diagonal basis randomly. For those bits where he and Alice coincidentally used the same bases, there should be

perfect correlation. If Alice sent out a bit 1 in rectilinear basis, meaning a polarization angle of 90° (see above table), and Bob also happens to measure it in the rectilinear basis, then he should measure an angle of 90° and interpret the bit as 1.

Alice and Bob then announce over a public (insecure) channel what bases they used for each bit measurement. They then discard those bits where they happened to have used *different* bases. In the case of the remaining bits, where they accidentally used the *same* bases, Alice can predict perfectly what bit value Bob should have measured each time. She sent those bits out and Bob's measurement scheme was correct by happenstance; so there should be perfect agreement. Similarly Bob can predict what bits Alice sent out, because he measured them and he knows that he measured them correctly. The only exception to this happens if an eavesdropper (named Eve) is lurking in the channel and disturbed the polarizations in her attempt to eavesdrop on the bits Alice was sending out. We will show in the next section that quantum mechanics (or more precisely the Heisenberg uncertainty principle and the no cloning theorem) guarantees that this disturbance must take place whenever Eve intercepts a photon.

Alice now announces over a public channel *some* of the bits she sent out and asks Bob to check if he received those particular bits intact. If he did, then there is likely to be no eavesdropper and the channel is secure. Any disagreement between the values of the bits Alice sent out and Bob measured correctly (with the same basis) reveals the presence of an eavesdropper who caused a disturbance. In the quantum world, Eve cannot hide since she cannot avoid causing a disturbance whenever she tries to eavesdrop on the bits.

Here is why Eve causes a disturbance. In her attempt to eavesdrop, she must intercept the bits from Alice before they reach Bob and measure the polarizations to decipher the bits. Since she does not know what bases Alice used to encode the bits, she measures them in random bases. Let us consider the situation when Alice sent out a bit with value 1 in the rectilinear basis and Eve measured it in the diagonal basis. Because of the uncertainty relationship between the rectilinear and diagonal bases, Eve cannot tell whether the bit was 0 or 1. In her attempt to hide, she must send a photon out to Bob pretending to be Alice. One half of the time she will send out the incorrect bit 0 in the rectilinear basis (this is also the no-cloning theorem; she can never clone the photon's polarization - a quantum entity - with 100% fidelity). Let us say now that Bob measures this in the rectilinear basis and measures a 0 because that is what he received from Eve. Later, when Bob and Alice compare notes over this bit, they will realize that Alice sent a bit with value

1 but Bob received a 0. Therefore, this disagreement reveals the presence of Eve.

Of course, just a few disagreements do not reveal the presence of Eve since they could be due to imperfections in the channel or other errors that cause bit flips. However, consistent disagreements in several bits reveal the presence of Eve. In fact, the probability of detecting Eve goes as $1 - (3/4)^n$ where n is the number of bits tested. Thus, Eve can be detected with near unit probability by testing a large number of bits. Once Eve is detected, Alice and Bob stop communicating and try again later. This goes on till Eve gets bored and leaves.

In this section, we showed that quantum mechanics guarantees secure cryptography. In 1989, IBM built a quantum cryptography machine [95]. Today, there is a 30 km long quantum cryptography line operating under Lake Geneva in Switzerland [96].

16 Quantum teleportation

Anybody familiar with the popular sci-fi series Star Trek knows what teleportation is supposed to do. It takes an object (a human or a klingon in Star Trek), destroys it at the source, and recreates it *exactly* at the destination. The object does not traverse the intervening distance and hence the speed of teleportation, in principle, need not be restricted by the speed of light.

In the classical world of today, if we want to transmit an object such as this page to a reader some distance away, we will probably use a facsimile machine. This is very different from teleportation in two ways: first, the original is not destroyed at the source, and second, what is received at the destination cannot be an *exact* replica. It cannot be exact because of quantum mechanics. No matter how sophisticated the facsimile machine is, the individual lettering in this page is made up of atoms and sub-atomic particles. When the light from the facsimile machine shines on them to determine their exact position on the page, they impart them with a random momentum which will displace them randomly. This is Heisenberg's uncertainty principle at work which states that it is impossible to specify simultaneously two quantities whose operators do not commute, such as position and momentum, precisely. Thus, the lettering that is transmitted is never exactly what was fed to the facsimile machine. There must be some distortion.

What is true of a classical object such as this page of text, is even more true of a quantum object. Generally speaking, it is impossible to measure all the attributes of a quantum state simultaneously and exactly. Therefore, it is impossible to clone a quantum object. This is the basis of the *quantum*

no-cloning theorem.

Even though quantum mechanics forbids cloning or copying, it does not forbid teleportation where the original object is sent *absolutely intact* to the destination, but is then unavailable (effectively destroyed) at the source. Achieving this feat requires the use of Einstein-Podolsky-Rosen pairs which are twin quantum objects that are forever correlated in some way. This correlation or “entanglement” can occur if the two quantum objects have interacted at some time in the past.

Albert Einstein, Boris Podolsky and Nathan Rosen (henceforth called EPR) came up with the following gedanken experiment to question the validity of quantum mechanics [97]. Imagine the two electrons of a hydrogen molecule. These two electrons have interacted to form the molecule and are in the bonding state where their spins are known to be anti-parallel (singlet state). Now, an explosion rips the molecule apart and sends one electron to New York and the other to Tokyo. At this time, we know that the two electrons have opposite spins, but we do not know which one has upspin (measured in some basis) and which one has downspin. We will now attach labels to the two electrons (electrons are still treated as equals and indistinguishable particles) and denote the Tokyo electron with subscript 1 and the New York electron with subscript 2. The “spin part” of the actual two electron wave function must then be written as

$$\psi = \frac{1}{\sqrt{2}}(|\uparrow_1\downarrow_2\rangle \pm |\downarrow_1\uparrow_2\rangle) \quad (50)$$

This wave function indicates that either the Tokyo electron’s spin is “up” and the New York electron’s spin is “down”, or vice versa. These two possibilities have exactly the same probability. Note that even though we do not know the spin of either electron, we know that they are always anti-parallel. Therefore, the spins of these two electrons, separated by the vast Pacific Ocean, have become entangled like Siamese twins.

EPR was interested in a paradox that questioned the completeness of quantum theory. Let us concentrate on the electron in Tokyo and forget about the one in New York for a moment. The spin part of the Tokyo electron’s wave function is aptly written as

$$\psi_{Tokyo} = \frac{1}{\sqrt{2}}(|\uparrow_1\rangle \pm |\downarrow_1\rangle) \quad (51)$$

That is, its spin has equal probability of being “up” and “down”. Now, let us say, we measure the spin in New York using a Stern Gerlach apparatus and find it to be “up”. We will immediately know that the Tokyo electron’s spin is “down”. We have therefore collapsed the Tokyo electron’s spin wave

function (given by equation 51) to the “down” state, and at the same time, received information about the spin (namely , that it is “down”), by performing a measurement in New York. The information about the Tokyo electron’s spin has therefore traveled to New York instantaneously with infinite speed thereby breaking the light speed barrier. EPR argued that this is impossible and therefore quantum mechanics must be incomplete.

To remedy the situation, it was proposed that there must be local hidden variables in quantum mechanics which, when properly accounted for, can solve this conundrum. But in 1964, Bell proved a mathematical inequality, that showed that there are no *local* hidden variables in quantum mechanics [98]. However, there can be *non-local* hidden variables that could allow violation of Bell’s inequality and reconcile the EPR paradox with quantum mechanics. In 1982, Aspect, Dalibard and Roger, demonstrated the violation of Bell’s inequality using entangled photon pairs (whose polarizations are entangled), thereby demonstrating non-local hidden variables. Collapse of the wave function is a very unique type of interaction that is non-local unlike the known forces in nature (electroweak, gravity, and strong interactions). The predictions of quantum mechanics have never been proven false.

16.1 Entangled states

Mathematically, the wave functions of the entangled state of two particles are such that they cannot be written as the product of the wave functions of each particle. Recall the EPR spin pairs in New York and Tokyo. The wave function of the Tokyo electron’s spin is given by Equation 51 and similarly the wave function of the New York electron’s spin will be given by

$$\psi_{Tokyo} = \frac{1}{\sqrt{2}}(|\uparrow_2\rangle \pm |\downarrow_2\rangle) \quad (52)$$

Note that the product of Equation 51 and 52 does not yield Equation 50. The wave function of the entangled state of two objects cannot be written as the product of the wave functions of each one of them.

16.2 Teleporting a single qubit

In 1993, Charles Bennet and his co-workers showed how entangled EPR pairs can be used to teleport a quantum object or more correctly, the quantum attribute of an object, over arbitrary distances

[99]. This will not allow us to teleport an entire electron physically, but we can teleport its *spin state* to another electron at a remote location. Since electrons are indistinguishable particles, this is indeed tantamount to teleporting the electron.

Consider the case where a qubit is encoded in the spin of a single electron (particle 1). The spin wave function or qubit is written as

$$\phi_1 = a|\uparrow_1\rangle + b|\downarrow_1\rangle = \begin{pmatrix} a \\ b \end{pmatrix} \quad (53)$$

where $|a|^2 + |b|^2 = 1$.

To teleport this object from a sender Alice to a receiver Bob, we will need Alice and Bob to have shared in the past an EPR pair which we will call particles 2 and 3. Particle 2 is with Alice and particle 3 resides with Bob. Their joint state wave function can be written as Equation 50 with just the labels altered.

$$\phi_{23} = \frac{1}{\sqrt{2}}(|\uparrow_2\downarrow_3\rangle - |\downarrow_2\uparrow_3\rangle) \quad (54)$$

At this point, particle 1 is still uncorrelated with particles 2 and 3. Therefore, we can write the three-particle (or three-spin) wave function as a product between ϕ_1 and ϕ_{23}

$$\begin{aligned} \phi_{123} &= \phi_1 \otimes \phi_{23} \\ &= \phi_1 \otimes \frac{1}{\sqrt{2}}(|\uparrow_2\downarrow_3\rangle - |\downarrow_2\uparrow_3\rangle) \\ &= \frac{a}{\sqrt{2}}(|\uparrow_1\rangle \otimes |\uparrow_2\rangle \otimes |\downarrow_3\rangle - |\uparrow_1\rangle \otimes |\downarrow_2\rangle \otimes |\uparrow_3\rangle) \\ &\quad + \frac{b}{\sqrt{2}}(|\downarrow_1\rangle \otimes |\uparrow_2\rangle \otimes |\downarrow_3\rangle - |\downarrow_1\rangle \otimes |\downarrow_2\rangle \otimes |\uparrow_3\rangle) \end{aligned} \quad (55)$$

Alice now makes a so-called Bell measurement to entangle the qubit (particle 1) with her particle 2. She lowers the potential barriers separating particles 1 and 2 and makes their wave functions overlap in space. The subsequent Bell measurement will involve measuring the total spin of particles 1 and 2, and the symmetry of the spatial parts of their coupled wave functions, that is whether the spatial part is symmetric in space or anti-symmetric. Typically, the symmetric eigenstate will have lower energy than the anti-symmetric eigenstate so that a measurement of the energy eigenstate is effectively a measurement of the spatial symmetry.

The wave function of the joint states of particles 1 and 2 after they are entangled (i.e. after their wave functions are made to overlap) can have one of only four forms. They can be written as

$$\psi_A = \frac{1}{\sqrt{2}}(|\uparrow_1\downarrow_2\rangle - |\downarrow_1\uparrow_2\rangle)$$

$$\begin{aligned}
\psi_B &= \frac{1}{\sqrt{2}}(|\uparrow_1\downarrow_2\rangle + |\downarrow_1\uparrow_2\rangle) \\
\psi_C &= \frac{1}{\sqrt{2}}(|\uparrow_1\uparrow_2\rangle - |\downarrow_1\downarrow_2\rangle) \\
\psi_D &= \frac{1}{\sqrt{2}}(|\uparrow_1\uparrow_2\rangle + |\downarrow_1\downarrow_2\rangle)
\end{aligned} \tag{56}$$

These states are called Bell basis states and they are mutually orthogonal. Note that the first two states are singlet and the last two are triplet. Hence a measurement of total spin will separate these two subgroups. Then within each subgroup, one state is symmetric in spin and the other is antisymmetric. Since the total two-body wave function (spin + spatial part) must be antisymmetric, a symmetric state in spin implies that the spatial part of the wave function must be anti-symmetric and vice versa. Thus measurement of the symmetry of the spatial part and the total spin is sufficient to identify the actual state among the four given in Equation 56. The purpose of Alice's Bell measurement is to complete this unambiguous identification.

Using Equation 56, we can re-write Equation 55 as

$$\begin{aligned}
\phi_{123} &= \frac{1}{2}[\psi_A(-a|\uparrow_3\rangle - b|\downarrow_3\rangle) + \psi_B(-a|\uparrow_3\rangle + b|\downarrow_3\rangle) \\
&+ \psi_C(a|\downarrow_3\rangle + b|\uparrow_3\rangle) + \psi_D(a|\downarrow_3\rangle - b|\uparrow_3\rangle)]
\end{aligned} \tag{57}$$

Using the column vector notation of Equation 53, we can re-write the above equation as

$$\phi_{123} = \frac{1}{2} \left[\psi_A \begin{pmatrix} -a \\ -b \end{pmatrix}_3 + \psi_B \begin{pmatrix} -a \\ b \end{pmatrix}_3 + \psi_C \begin{pmatrix} b \\ a \end{pmatrix}_3 + \psi_D \begin{pmatrix} -b \\ a \end{pmatrix}_3 \right] \tag{58}$$

The 3-particle state is now such that if Alice's Bell measurement reveals that particles 1 and 2 are in state ψ_A , then Bob's particle 3 encodes the qubit $(-a|\uparrow\rangle - b|\downarrow\rangle)$. if Alice's measurement reveals the state ψ_B , then Bob's particle 3 encodes the qubit $(-a|\uparrow\rangle + b|\downarrow\rangle)$, if Alice's measurement reveals the state ψ_C , then Bob's particle 3 encodes the qubit $(b|\uparrow\rangle + a|\downarrow\rangle)$, and finally if Alice's measurement reveals the state ψ_D , then Bob's particle 3 encodes the qubit $(-b|\uparrow\rangle + a|\downarrow\rangle)$.

After the Bell measurement, Alice will know how the state of Bob's particle 3 is related to the original qubit (particle 1), but Bob does not. So Alice must send Bob the result of the Bell measurement. Since there are four possible outcomes of the Bell measurement, Alice needs to send Bob two classical bits telling him which outcome was observed. Accordingly, Bob applies a unitary transformation to particle 3 to re-create particle 1 and hence the qubit. These unitary

transformations are

$$\begin{aligned}
 \psi_A &\rightarrow \begin{pmatrix} -1 & 0 \\ 0 & -1 \end{pmatrix} \\
 \psi_B &\rightarrow \begin{pmatrix} -1 & 0 \\ 0 & 1 \end{pmatrix} \\
 \psi_C &\rightarrow \begin{pmatrix} 0 & 1 \\ 1 & 0 \end{pmatrix} \\
 \psi_D &\rightarrow \begin{pmatrix} 0 & -1 \\ 1 & 0 \end{pmatrix}
 \end{aligned} \tag{59}$$

Note that since Alice must send Bob 2 classical bits to help him transform his particle 3 to particle 1, particle 1 was not teleported to Bob instantly. There was no superluminal signaling. The classical bits must travel to Bob with speed equal to or less than the speed of light in vacuum. There is one subtle exception however. One fourth of the time (corresponding to ψ_A), Bob does not have to apply any transformation (apart from an irrelevant phase factor of π) to his particle 3 in order to re-create particle 1. Therefore, if Alice and Bob are content to live with a 25% success rate, instant teleportation is possible. It does not violate relativistic dictates since no definite information is being transmitted. In fact, the 25% teleportation has been demonstrated experimentally by Zeilinger’s group in Austria.

17 Quantum memory

No review article is ever complete. But this review will be seriously amiss if we do not mention a few words about quantum “memory”. Most of the attention in the field of quantum computing has be focused on quantum logic, and very little on quantum memory.

Quantum memory is an important constituent of quantum information science. It has many applications: (i) increasing the efficiency of quantum key distribution (QKD) protocols (the receiver Bob stores the received qubits in a quantum memory and measures them *after* the sender Alice tells him the bases), (ii) improving the EPR-based QKD schemes [100], (iii) teleporting a state using singlet pairs prepared in advance, (iv) new schemes for QKD that rely on the existence of short-term memory [101, 102], (v) attacking oblivious transfer and quantum bit commitment schemes [103], etc.

The requirements for quantum memory are thought to be very different from those of quantum gates. In a quantum gate, the qubits are accessed and rotated numerous times, but the coherence time need not be very long; it simply has to be much longer than the switching time. In contrast, the qubits in a quantum memory are seldom accessed, but they must live much longer (ideally “forever”) without decohering. One must also be able to access them with high fidelity.

Since this review has focused on spintronic solid-state realizations of quantum logic, we will stick to the spintronic solid state realization of quantum memory. This is no easy task since spin coherence times, although longer than charge coherence times, are still very short. As a result, *non-volatile* quantum static memories (Q-SRAMs) are not appropriate; rather, quantum *dynamic memories* (Q-DRAMs) may be possible if the qubit can be *refreshed* periodically through refresh cycles. Below, we explore possible routes to refreshing the quantum state of a quanton [55].

17.1 Refreshing a qubit

It is very possible that refreshing can be accomplished through the *quantum Zeno effect* which postulates that repeated observations of a qubit will inhibit its decay [104, 106]. Repeated observations automatically serve as refresh cycles. However, this repeated observation has to be carried out by a non-invasive detector. A ballistic point contact has been used in the past as a non-invasive charge detector for electrons in quantum dots [105], and its role in the context of the quantum Zeno effect has been examined [106]. It may be possible to use a spin-polarized scanning tunneling microscope tip as a non-invasive probe for spin, but that is yet to be realized in practice.

But what happens if the probe is an “invasive” probe? All is not lost. It may be possible to re-create the entire qubit (including the phase) after it has “interacted” with the probe. This involves *quantum erasure* [107, 108, 109] as explained below.

Consider a quanton in a coherent superposition of two spin states, described by a wave function

$$\psi = a_{\uparrow}|\uparrow\rangle + a_{\downarrow}|\downarrow\rangle \tag{60}$$

A fundamental result of quantum measurement theory is that if the spin analyzer tries to detect the spin of the incoming quanton, the interaction between the detector and the quanton causes the wave function of the detector to become entangled with that of the quanton. The entangled (non-factorizable) wave function is

$$\Phi = a_{\uparrow}|\uparrow\rangle|1\rangle + a_{\downarrow}|\downarrow\rangle|2\rangle \tag{61}$$

where the wave functions $|1\rangle$ and $|2\rangle$ span the Hilbert space of the detector. Thus, $|1\rangle$ corresponds to the detector (spin-analyzer) passing an up-spin quanton, and $|2\rangle$ corresponds to the detector reflecting a downspin quanton.

If we make a measurement of whether the detector passed the quanton (corresponding to the determination that the quanton's spin was "up"), the probability amplitude of that is

$$\Psi = \langle 1 | \Phi \rangle = a_{\uparrow} | \uparrow \rangle \langle 1 | 1 \rangle + a_{\downarrow} | \downarrow \rangle \langle 1 | 2 \rangle \quad (62)$$

Since the detector makes an "unambiguous" determination, meaning that it *always* passes an upspin quanton and *never* passes a downspin quanton, the wave functions $|1\rangle$ and $|2\rangle$ are orthogonal, meaning that upspin detection and downspin detection are mutually exclusive (a quanton cannot be simultaneously both upspin and downspin, and the detector will unambiguously determine what the spin is). Hence, from Equation (62),

$$\Psi_{detected} = a_{\uparrow} | \uparrow \rangle; \quad |\Psi|^2 = |a_{\uparrow}|^2 \quad (63)$$

and we get no information about a_{\downarrow} , or the phase. This is interpreted as wave function collapse. However, the entanglement of the detector with the quanton (Equation (61)) does not itself cause irreversible collapse. It is not irreversible since if we design an experiment whose result is the probability of a particular outcome of the spin measurement *and* finding the detector in the symmetric state ($|1\rangle + |2\rangle$), then the corresponding probability amplitude is

$$\begin{aligned} [\langle 1 | + \langle 2 |] | \Phi \rangle &= a_{\uparrow} | \uparrow \rangle \langle 1 | 1 \rangle + a_{\downarrow} | \downarrow \rangle \langle 1 | 2 \rangle + a_{\downarrow} | \downarrow \rangle \langle 2 | 2 \rangle + a_{\uparrow} | \uparrow \rangle \langle 2 | 1 \rangle \\ &= a_{\uparrow} | \uparrow \rangle + a_{\downarrow} | \downarrow \rangle \\ &= \psi, \end{aligned} \quad (64)$$

which is the original wave function. Hence, we can restore the original wave function ψ from the entangled wavefunction Φ . This is possible since Equation (61) still represents a "pure" state and not a "mixed" state.

Note that if we can find the detector in the symmetric state, we would not have known whether the quanton that passed through it was "up" or "down", and hence we would not have collapsed the wave function. Thus, by finding the detector in the symmetric state, we have foregone any information about the spin and hence restored the original coherent superposition state from the entangled state (quanton entangled with detector). The quantum erasure is possible because the entangled wave function Φ is still a pure state and not a mixed state.

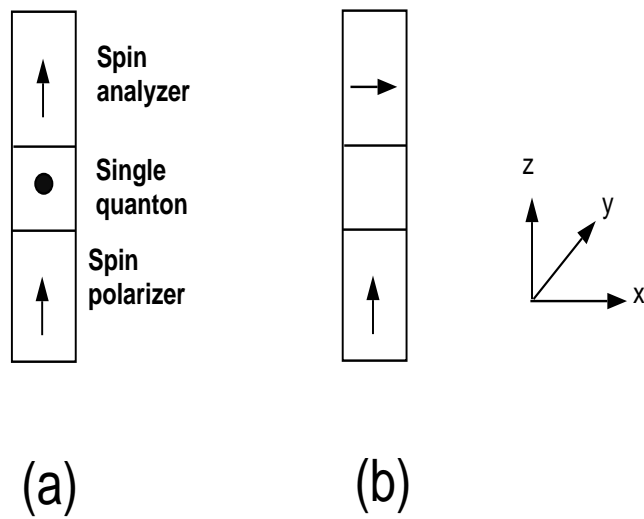


Figure 10: The (a) initial and (b) final state of the polarizer-analyzer combination after the passage of a quanton corresponding to the reading of a qubit. Reproduced from ref. [55] with permission of the Electrochemical Society.

What do we need to implement quantum erasure? We need only one difficult and ambitious technological feat. When the quanton passes through the spin analyzer, it should be able to rotate the magnetization of the analyzer and *change it* in a particular way. If the polarizer and analyzer were originally magnetized in the +z-direction, the passage of the quanton through the analyzer must turn on some interaction that results in the analyzer getting magnetized in the +x-direction. Fig. 10 depicts this situation. We assume that $|1\rangle$ corresponds to the state of the detector whereby the analyzer is magnetized (spin polarized) in the +z-direction and $|2\rangle$ corresponds to the state of the detector whereby the analyzer is magnetized in the -z-direction. Thus,

$$|1\rangle \rightarrow \begin{bmatrix} 1 \\ 0 \end{bmatrix} \quad (65)$$

$$|2\rangle \rightarrow \begin{bmatrix} 0 \\ 1 \end{bmatrix} \quad (66)$$

Clearly $|1\rangle$ and $|2\rangle$ are orthogonal and the state $|1\rangle + |2\rangle$ corresponds to the state

$$|1\rangle + |2\rangle \rightarrow \begin{bmatrix} 1 \\ 1 \end{bmatrix}, \quad (67)$$

which corresponds to spin-polarization in the +x-direction.

Thus, we must find the analyzer polarized in the +x-direction after the quanton passes through it. In other words, the magnetization of the analyzer must be sensitive to the passage of a quanton and respond to it. At present, this is not possible; but the recent discovery of control of magnetization via an electric current in InMnAs [110] may one day lead to a practical paradigm for achieving this.

18 Conclusions

In this review article, I have provided a bird's eye view of the current status of quantum information science from the perspective of a device engineer. This is one of the fastest growing fields judging by the number of new journals that are appearing with amazing frequency to disseminate many of the important new findings. This field will continue to grow and my only regret is that when this article appears in print it would probably have been already outdated.

19 Acknowledgement

My interest in quantum computing was kindled at the Quantum Devices and Circuits conference held in Alexandria, Egypt in 1996 which I co-organized. That conference included presentations by some of the pioneers in this field including Charles Bennet and Umesh Vazirani. I learnt a lot from my friend and colleague Prof. Vwani Roychowdhury of UCLA. The quantum dot realization of the Toffoli-Fredkin gate is the work of my ex-student Prof. Alexander Balandin of the University of California-Riverside during his tenure as a post-doctoral advisee in my group. I also acknowledge fruitful discussions with my colleagues Professors Frazer Williams, Natale Ianno and David Sellmyer of my erstwhile institution, the University of Nebraska-Lincoln with which I will always have a special connection. I have benefitted from discussions with Prof. David Janes of Purdue University and Dr. Berry Jonker of the Naval Research Laboratory regarding fabrication and MBE growth. The work in spintronics is carried out in collaboration with Prof. Marc Cahay of the University of Cincinnati.

My work in quantum computing has been supported by the Nebraska Research Initiative in Quantum Information Processing and the National Science Foundation.

This article is dedicated to the memory of Dr. Rolf Landauer whose work in this field has taught me much.

Appendix: Rashba Effect in a Quantum Dot

In this appendix, we will derive the total spin-splitting in a quantum dot capped by ferromagnetic contacts. Consider the system shown in Fig. 11. The ferromagnetic contacts give rise to an in-built magnetic field in the x-direction which can be quite strong in realistic structures (~ 1 Tesla). There may be an electric field in the x-direction as well to maintain single electron occupancy and an electric field in the y-direction to induce the Rashba effect.

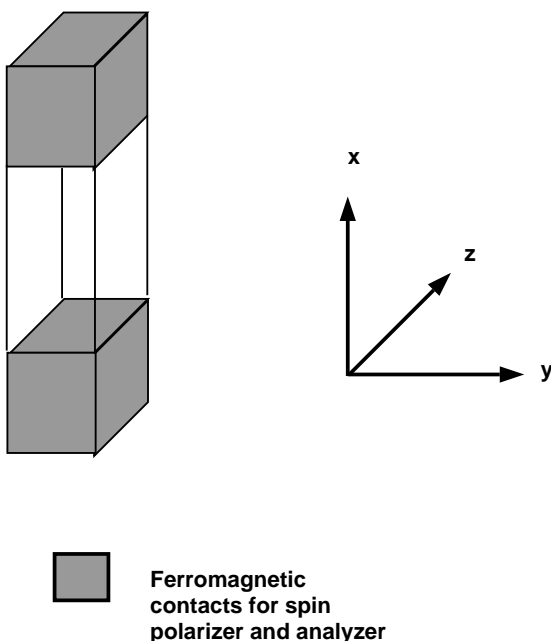


Figure 11: The geometry of a semiconductor quantum dot capped by ferromagnetic contacts. The contacts induce a magnetic field in the x-direction, which in turn, induces a Zeeman splitting of the subband levels in the semiconductor quantum dot. The dot does not have hardwall boundaries. Consequently, the wave functions of the spin split levels leak out into the adjoining barrier. The eigenstate of the spin aligned against the magnetic field has a higher energy and hence its wave function leaks out more into the barrier compared to the wave function of the spin aligned along the magnetic field.

The total Hamiltonian for an electron in the semiconductor layer is

$$\begin{aligned} H &= \frac{(\vec{p} - e\vec{A})^2}{2m^*} - e\mathcal{E}_x x - e\mathcal{E}_y y + (g/2)\mu_B B_x \sigma_x + H_R \\ &= H_0 + H_R \end{aligned} \quad (68)$$

where g is the Landé g-factor, e is the electronic charge, μ_B is the Bohr magneton, σ_x is the x-component of the Pauli spin matrix, and H_R is the Rashba interaction given by

$$H_R = i \frac{\hbar^2}{2m^{*2}c^2} \nabla V \cdot [\vec{\sigma} \times \vec{\nabla}] = \frac{e\hbar}{2m^{*2}c^2} \vec{\mathcal{E}} \cdot \vec{\sigma} \times \vec{p} \quad (69)$$

where $\vec{\sigma}$ is the Pauli spin matrix, \vec{p} is the momentum operator, and $\vec{\mathcal{E}}$ is the electric field inducing the Rashba effect.

We will neglect the effect of the x-directed electric field on the Rashba effect and include only the effect of the y-directed field which is much larger since the potential applied along the x-direction must be smaller than $e/2C$ to maintain Coulomb blockade. In any case, the x-directed field has no Rashba effect on x-polarized spins, and we are interested in the energy splitting between the +x and -x-polarized spins. Therefore,

$$H_R = \frac{e\hbar}{2m^{*2}c^2} \mathcal{E}_y [\sigma_z p_x - \sigma_x p_z] \quad (70)$$

The Zeeman term $(g/2)\mu_B B_x \sigma_x$ introduces an Zeeman splitting between the +x-polarized spin ($|\uparrow\rangle$) and the -x-polarized spin ($|\downarrow\rangle$). If the potential confining the electron in the semiconductor quantum dot is finite (the conduction band offset between the semiconductor and the surrounding material is finite), then the spatial parts of the “upspin” (+x-polarized) and “downspin” (-x-polarized) states are slightly different. The wave function of the higher energy state will be spread out a little bit more. This is shown in Fig. 1(d). Thus, if the downspin state is at a higher energy, then the spatial parts of the wave functions of the two spin states in the lowest spin-split subband of the quantum dot can be written as

$$\begin{aligned} \phi_{\uparrow} &= \left(\frac{2\sqrt{2}}{\sqrt{W_x W_y W_z}} \right) \sin\left(\frac{\pi x}{W_x}\right) \sin\left(\frac{\pi y}{W_y}\right) \sin\left(\frac{\pi z}{W_z}\right) \\ \phi_{\downarrow} &= \left(\frac{2\sqrt{2}}{\sqrt{W'_x W'_y W'_z}} \right) \sin\left(\frac{\pi x}{W'_x}\right) \sin\left(\frac{\pi y}{W'_y}\right) \sin\left(\frac{\pi z}{W'_z}\right) \end{aligned} \quad (71)$$

where $W'_x > W_x$, $W'_y > W_y$ and $W'_z > W_z$. These widths are larger than the physical dimensions of the quantum dot since the wave functions will leak out into the barrier as long as the barrier is

not of infinite height. The point of this exercise is to show that the spatial parts of the two spin states are different because of the Zeeman splitting. This is a critical requirement for the Rashba splitting.

Next, we will evaluate the total spin splitting (Δ) which is a combination of the Zeeman and Rashba splitting. The latter can be modulated by the transverse gate potential.

The time-independent Schrödinger equation describing the ground state of the system is

$$(H_0 + H_R)\psi = E\psi \quad (72)$$

We will expand ψ in the basis functions of the two lowest spin-resolved subband states. We can neglect the higher subband states as long as the Rashba spin splitting Δ_R is much smaller than the energy separation between the lowest two subbands in the quantum dot. If the effective mass is equal to the free electron mass and the dimensions of the quantum dot in all directions is about 10 nm, then the energy separation between the two lowest subbands is 33 meV. This is obviously much larger than any reasonable Rashba splitting which scarcely exceeds 1 meV. Hence, neglecting the higher subbands is justified.

Hence

$$\psi = a_\uparrow\phi_\uparrow + a_\downarrow\phi_\downarrow \quad (73)$$

Using the above in Equation 72, we get

$$\begin{bmatrix} \langle H_1 \rangle + \langle H_R \rangle_{11} & \langle H_R \rangle_{12} \\ \langle H_R \rangle_{21} & \langle H_2 \rangle + \langle H_R \rangle_{22} \end{bmatrix} \begin{pmatrix} a_\uparrow \\ a_\downarrow \end{pmatrix} = E_{ground} \begin{pmatrix} a_\uparrow \\ a_\downarrow \end{pmatrix}, \quad (74)$$

where $\langle H_1 \rangle = \langle \phi_\uparrow | H_0 | \phi_\uparrow \rangle$, $\langle H_2 \rangle = \langle \phi_\downarrow | H_0 | \phi_\downarrow \rangle$, $\langle H_R \rangle_{11} = \langle \phi_\uparrow | H_R | \phi_\uparrow \rangle$, $\langle H_R \rangle_{22} = \langle \phi_\downarrow | H_R | \phi_\downarrow \rangle$, $\langle H_R \rangle_{12} = \langle \phi_\uparrow | H_R | \phi_\downarrow \rangle$, and $\langle H_R \rangle_{21} = \langle \phi_\downarrow | H_R | \phi_\uparrow \rangle$.

Diagonalizing the above Hamiltonian, we get that the total splitting between the upspin and downspin states is

$$\begin{aligned} E_\downarrow - E_\uparrow &= 2\sqrt{\left(\frac{\langle H_1 \rangle - \langle H_2 \rangle + \langle H_R \rangle_{11} - \langle H_R \rangle_{22}}{2}\right)^2 + \langle H_R \rangle_{12}\langle H_R \rangle_{21}} \\ &= 2\sqrt{\left(\frac{g\mu_B B}{2} + \frac{e\hbar}{2m^*c^2}\mathcal{E}_y \langle p_x \rangle\right)^2 + \left|\frac{e\hbar}{2m^*c^2}\mathcal{E}_y \langle p_z \rangle\right|^2} \end{aligned} \quad (75)$$

where $\langle p_x \rangle = \langle \phi_\uparrow | -i\hbar(\partial/\partial x) | \phi_\uparrow \rangle = \langle \phi_\downarrow | -i\hbar(\partial/\partial x) | \phi_\downarrow \rangle = 0$ and $\langle p_z \rangle = \langle \phi_\uparrow | -i\hbar(\partial/\partial z) | \phi_\downarrow \rangle = \frac{8i\hbar}{\sqrt{W_z W'_z}} \cos^2\left(\frac{\pi W_x}{2 W'_x}\right)$.

Therefore the total splitting is

$$\Delta = E_{\downarrow} - E_{\uparrow} = 2\sqrt{\left(\frac{g\mu_B B}{2}\right)^2 + \mathcal{E}_y^2 \frac{16e^2\hbar^4}{m^*4c^4W_xW'_x} \cos^4\left(\frac{\pi W_x}{2W'_x}\right)} \quad (76)$$

The last term under the radical is the Rashba effect which can be varied by the electric field \mathcal{E}_y . Note that this term would have vanished if $W_x = W'_x$, that is, if the spatial parts of the upspin and downspin wave functions were identical. Here, we have made the spatial parts different by using a finite potential barrier and a magnetic field to raise the energy of the downspin state above that of the upspin state.

We can estimate the magnitude of the Rashba splitting in realistic systems. Assuming $W_x = 10$ nm, $W'_x = 11$ nm, $\mathcal{E}_y = 10^7$ V/m, $B = 1$ Tesla, $g = 2$, we find that increasing the electric field from 10^7 V/m to twice that value increases the Rashba splitting by about $1.5 \mu\text{eV}$. Thus, the modulation of the splitting is very small.

References

- [1] J. Church, (1936) *Amer. J. Math.*, **58**, 435.
- [2] A. M. Turing, (1936) *Proc. London Math Soc. Ser. 2*, **442**, 230.
- [3] R. Maeder, (1993) *The Mathematica Journal*, **3**, 36.
- [4] J. Gill, (1977) *SIAM J. Comput.*, **6**, 675.
- [5] C. Bennett, (1973) *IBM J. Res. Develop.*, **17**, 525.
- [6] P. Benioff, (1980) *J. Stat. Phys.*, **22**, 563.
- [7] R. P. Feynman, (1982) *Int. J. Theor. Phys.*, **21**, 467.
- [8] D. Deutsch, (1985) *Proc. Royal Soc. London*, **A400**, 97.
- [9] R. Josza, (1991) *Proc. Royal Soc. London*, **A435**, 563.
- [10] D. Deutsch and R. Josza, (1992) *Proc. Royal Soc. London*, **A439**, 553.
- [11] P. W. Shor (1996) in *Proc. 37th Ann. Symp. Foundations of Comp. Sci.*, IEEE Computer Society Press, pp. 56-65.
- [12] Colin P. Williams and Scott H. Clearwater, *Explorations in Quantum Computing*, (Springer-Verlag, New York, 1998).
- [13] R. Silverman, (1987) *Mathematical Computing*, **48**, 329.
- [14] R. Crandall, *Topics in Advanced Scientific Computation* (Springer-Verlag, New York, 1996), p. 125.
- [15] R. Rivest, A. Shamir and L. Adelman, (1978) *Commun. of the ACM*, **21**, 120.
- [16] A. Kitaev, (1997) *Russian Math Surveys*, **52**, 1191.
- [17] L. K. Grover, (1997) *Phys. Rev. Lett.*, **79**, 325; *ibid* (1997) **79**, 4709.
- [18] C. Durr and P. Hoyer, (1996) Los Alamos pre-print archive, xxx.lanl.gov/archive/quant-ph/9612003.

- [19] The Semiconductor Industry Association National Technology Roadmap, 1994.
- [20] D. B. Tuckerman and R. F. W. Pease, (1981) *IEEE Electron Dev. Lett.*, **2**, 126.
- [21] R. Landauer, (1961) *IBM J. Res. Develop.*, **5**, 183; R. W. Keyes and R. Landauer, (1970) *ibid*, **14**, 152.
- [22] A. N. Korotkov in *Extended Abstracts of the 1997 International Conference on Solid State Devices and Materials*, Hamamatsu, Japan, pp. 304-305; A. N. Korotkov in *Molecular Electronics*, eds. J. Jortner and M. A. Ratner (Blackwell, Oxford, 1997).
- [23] Vwani Roychowdhury, private communication.
- [24] E. Fredkin and T. Toffoli, (1982) *Int. J. Theor. Phys.*, **21**, 219.
- [25] S. Lloyd, (1993) *Science*, **261**, 1569; S. Lloyd, (1994) *Science* **263**, 695.
- [26] C. H. Bennett, (1982) *Int. J. Theor. Phys.*, **21**, 905.
- [27] C. H. Bennett and R. Landauer, (1985) *Sci. Am.*, **253**, 48.
- [28] T. Toffoli, in *Seventh Colloquium in Automata, Languages and Programming*, Eds. J. W. de Bakker and J. W. van Leeuwen, (Springer-Verlag, Berlin, 1980). p. 632.
- [29] K. K. Likharev, (1982) *Int. J. Theor. Phys.*, **21**, 311.
- [30] R. Landauer, in *Der Informationsbegriff in Technik und Wissenschaft*, Eds. O. G. Folberth and C. Hackl (R. Oldenbourg, München, 1986), p. 139.
- [31] K. K. Likharev and A. N. Korotkov, (1996) *Science*, **273**, 763.
- [32] S. Bandyopadhyay and V. P. Roychowdhury, (1997) *Superlat. and Microstruct.*, **22**, 411.
- [33] S. Bandyopadhyay, A. Balandin, V. P. Roychowdhury and F. Vatan, (1998) *Superlat. Microstruct.*, (Special Issue in Honor of Rolf Landauer on the Occasion of his 70th Birthday) **23**, 445.
- [34] D. Deutsch, (1992) *Physics World*, **5**, 57.
- [35] The author was made aware of this proof by Professor Vwani Roychowdhury.

- [36] D. P. DiVincenzo, (1995) *Phys. Rev. A*, **51**, 1015.
- [37] S. Lloyd, (1995) *Phys. Rev. Lett.*, **75**, 346.
- [38] N. Ashcroft and D. Mermin, *Solid State Physics* (Saunders College, Philadelphia, 1976).
- [39] S. S. Molotkov and S. N. Nazin, (1995) *JETP Lett.*, **62**, 272.
- [40] W. G. Unruh, (1995) *Phys. Rev. A*, **51**, 992.
- [41] R. T. Bate, in *VLSI Microstructure Science and Engineering*, Eds. N. G. Einspruch, Vol. 4, (Academic Press, New York, 1981).
- [42] C. Mead and L. Conway, *Introduction to VLSI Systems*, Chap. IX, (Addison-Wesley, Reading, Massachusetts, 1980). p. 333.
- [43] R. Landauer, (1982) *Int. J. Theor. Phys.*, **21**, 283 .
- [44] P. Benioff, (1982) *Int. J. Theor. Phys.*, **21**, 177.
- [45] W. G. Teich, K. Obermeyer and G. Mahler, (1988) *Phys. Rev. B*, **37**, 8111; W. G. Teich and G. Mahler, (1992) *Phys. Rev. A.*, **45**, 3300 ; H. Korner and G. Mahler, (1993) *Phys. Rev. B*, **48**, 2335.
- [46] .B. Lush, D.H. Levi, H.F. MacMillan, R.K. Ahrenkiel, M.R. Melloch, and M.S. Lundstrom, (1992) *Appl. Phys. Lett.*, **61**, 2440.
- [47] G.B. Lush, H.F. MacMillan, B.M. Keyes, D.H. Levi, M.R. Melloch, R.K. Ahrenkiel, and M.S. Lundstrom, (1992) *J. of Appl. Phys.*, **72**, 1436.
- [48] M.P. Patkar, M.S. Lundstrom, and M.R. Melloch,(1995) *J. of Appl. Phys.*, **78**, 2817 .
- [49] R.K. Ahrenkiel, B.M. Keyes, G.B. Lush, M.R. Melloch, M.S. Lundstrom, and H.F. MacMillan, (1992) *J. Vac. Sci. and Tech.*, **A10**, 990.
- [50] P. W. Shor, (1995) *Phys. Rev. A*, Vol. 52, No. 4, pp. 2493–2496.
- [51] A. M. Steane, (1996) *Phys. Rev. Lett.*, Vol. 77, No. 5, pp. 793–797.
- [52] A. R. Calderbank and P. W. Shor, (1996) *Phys. Rev. A*, Vol. 54, No. 2, pp. 1098–1105.

- [53] P. O. Boykin, T. Mor, M. Pulver, V. Roychowdhury and F. Vatan, (1999) LANL e-print quant-ph #9906054.
- [54] S. Bandyopadhyay, (2001) *Phys. Low Dim. Struct.*, **9/10**, 155.
- [55] S. Bandyopadhyay, in *Quantum Confinement VI: Nanostructured Materials and Devices*. Eds. M. Cahay, J-P Leburton, D. J. Lockwood, S. Bandyopadhyay and J. S. Harris, (The Electrochemical Society, Inc, Pennington, NJ, 2001), pp. 280-286.
- [56] S. Bandyopadhyay, (2001) *Physica E*, **11**, 126.
- [57] P. Mohanty, E. M. Q. Jariwalla and R. A. Webb, (1997) *Phys. Rev. Lett.*, **78**, 3366.
- [58] G. Feher, *Phys. Rev.*, (1959) **114**, 1219.
- [59] B. E. Kane, (1998) *Nature* (London), **393**, 133-137.
- [60] R. Vrijen, E. Yablonovitch, K. Wang. H. W. Jianh, A. Balandin, V. Roychowdhury, T. Mor and D. DiVincenzo, (2000) *Phys. Rev. A*, **62** 12306.
- [61] R. P. McKinnon, et. al., in *Proc. SPIE*, Vol. 4590 (BioMEMs and Smart Nanostructures Conference, Adelaide, Australia, December 2001).
- [62] V. Privman, I. D. Vagner and G. Kventsel, (1998) *Phys. Lett. A*, **239**, 141.
- [63] S. Bandyopadhyay, (2000) *Phys. Rev. B*, **61**, 13813.
- [64] G. Burkard, D. Loss and D. P. DiVincenzo, (1999) *Phys. Rev. B*, **59**, 2070.
- [65] J. M. Kikkawa and D. D. Awschalom, (1998) *Phys. Rev. Lett.*, **80**, 4313.
- [66] G. Lommer, F. Malcher, and U. Rössler, (1988) *Phys. Rev. Lett.*, **60**, 728-731.
- [67] E. I. Rashba, (1960) *Sov. Phys. Semicond.*, **2**, 1109-1122; Y. A. Bychkov and E. I. Rashba, (1984) *J. Phys. C*, **17**, 6039-6045.
- [68] C. Livermore, et. al., (1996) *Science*, **274**, 1332.
- [69] F. R. Waugh, et. al., (1995) *Phys. Rev. Lett.*, **75**, 705.
- [70] J. Nitta, T. Akazaki, H. Takayanagi, and T. Enoki, (1997) *Phys. Rev. Lett.* **78**, 1335-1339.

- [71] S. Datta and B. Das, (1990) *Appl. Phys. Lett.*, **56**, 665-667.
- [72] G. Schmidt, D. Ferrand, L. W. Molenkamp, A. T. Filip and B. J. van Wees, (2000) *Phys. Rev. B*, **62**, R4790.
- [73] E. I. Rashba, *Phys. Rev. B*, **62**, R16267 (2000).
- [74] P. R. Hammar, B. R. Bennett, M. J. Yang and M. Johnson, (1999) *Phys. Rev. B*, **83**, 203.
- [75] A. T. Hanbicki, O. M. J. van't Erve, R. Magno, G. Kioseoglou, C. H. Li, B. T. Jonker, G. Itskos, R. Mallory, M. Yasar and A. Petrou, *Appl. Phys. Lett.*, **82**, 4092 (2003); H. J. Zhu, M. Ramsteiner, H. Kostial, M. Waaermeier, H-P Schönber, and K. H. Ploog, *Phys. Rev. Lett.*, **87**, 016601 (2001); V. F. Motsnyi, J. De Boeck, J. Das, W. van Roy, G. Borghs, E. Goovaerts and V. I. Safarov, *Appl. Phys. Lett.*, **81**, 265 (2002); T. Manago and H. Akinaga, *Appl. Phys. Lett.*, **81**, 694 (2002); S. H. Chum, S. J. Potashnik, K. C. Ku, P. Schiffer and N. Samarth, *Phys. Rev. B*, **66**, R100408 (2002).
- [76] I. Malajovich, J. M. Kikkawa, D. D. Awschalom, J. J. Berry and N. Samarth, (2000) *Phys. Rev. Lett.*, **84**, 1015.
- [77] B. Muerer, D. Heitman and K. Ploog, (1988) *Phys. Rev. Lett.*, **68**, 1371.
- [78] M. Oestreich, J. Hübner, D. Hägele, P. J. Klar, W. Heimbrodt, W. W. Rühle, D. E. Ashenford and B. Lunn, (1999) *Appl. Phys. Lett.*, **74**, 1251-1253.
- [79] M. Devoret, D. Esteve, and C. Urbina, (1992) *Nature*, **360**, 547.
- [80] J. Fabian and S. Das Sarma, *J. Vac. Sci. Tech. B*, **17**, 1708 (1999).
- [81] R. J. Elliott, *Phys. Rev.*, **96**, 266 (1954).
- [82] A. W. Overhauser, *Phys. Rev.*, **89**, 689 (1953).
- [83] H. Benisty, C. M. Sotomayor-Torres and C. Weisbuch, *Phys. Rev. B*, **44**, 10945 (1991).
- [84] G. Dresselhaus, *Phys. Rev.*, **100**, 580 (1955).
- [85] S. Pramanik, S. Bandyopadhyay and M. Cahay, *Phys. Rev. B*, **68**, 075313 (2003).
- [86] M. I. D'yakonov and V. I. Perel, *Sov. Phys. JETP*, **33**, 1053 (1971).

- [87] S. I. Erlingsson, Y. V. Nazarov and V. I. Falko, *Phys. Rev. B*, **64**, 195306 (2001); A. V. Khaetskii, D. Loss and L. Glazman, *Phys. Rev. Lett.*, **88**, 186802 (2002); Y. B. Lyanda-Geller, I. L. Aleiner and B. L. Altshuler, *Phys. Rev. Lett.*, **89**, 107602 (2002); S. deSousa and S. Das Sarma, *Phys. Rev. Lett.*, **67**, 033301 (2003); S. Saykin, D. Mozyrsky and V. Privman, *NanoLetters*, **2**, 651 (2002); J. M. Taylor, C. M. Marcus and M. D. Lukin, *Phys. Rev. Lett.*, **90**, 206803 (2003); A. Imamoglu, E. Knill, L. Tian and P. Zoller, *Phys. Rev. Lett.*, **91**, 017402 (2003); Y. G. Semenov and K. W. Kim, *Phys. Rev. B*, **67**, 073301 (2003).
- [88] G. L. Bir, A. G. Aronov and G. E. Pikus, *Sov. Phys. JETP*, **42**, 705 (1976).
- [89] L. Fedichkin, A. Federov and V. Privman, “Additivity of Decoherence Measures for Multi-Qubit Quantum Systems”, www.arXiv.org/cond-mat/0309685.
- [90] H. X. Tang, F. G. Monzon, Ron Lifshitz, M. C. Cross and M. L. Roukes, (2000) *Phys. Rev. B*, **61**, 4437.
- [91] Y. Ohno, D. K. Young, B. Beschoten, F. Matsukura, H. Ohno and D. D. Awschalom, (1999) *Nature* (London), **402**, 790.
- [92] R. Fiederling, M. Keim, G. Reuscher, W. Ossau, G. Schmidt, A. Waag and L. W. Molenkamp, (1999) *Nature* (London), **402**, 787.
- [93] C. Bennet, F. Bessette, G. Brassard, F. Salvail and J. Smolin, (1992) *J. Cryptology*, **5**, 3.
- [94] C. Bennet, G. Brassard and A. Ekert, *Scientific American*, **50-57** October 1992.
- [95] C. Bennett and G. Brassard, *SIGACT News*, **20**, 78, Fall 1989.
- [96] C. Marand and P. Townsend, (1995) *Optics Letters*, **20**, 1695.
- [97] A. Einstein, B. Podolsky and N. Rosen, (1935) *Phys. Rev.*, **47**, 777.
- [98] J. Bell, (1964) *Physics*, **1**, 195.
- [99] C. Bennet, G. Brassard, C. Crepeau, R. Josza, A. Peres and W. Wootters, (1993) *Phys. Rev. Lett.*, **70**, 1895.
- [100] A. Ekert, (1991) *Phys. Rev. Lett.*, **67**, 661.

- [101] C. H. Bennet and S. J. Wiesner, (1992) *Phys. Rev. Lett.*, **69**, 2881.
- [102] L. Goldenberg and L. Vaidman, (1995) *Phys. Rev. Lett.*, **75**, 1239.
- [103] T. Mor, D.Sc. thesis, LANL e-print quant-ph/9900073.
- [104] B. Misra and E. C. G. Sudarshan, (1977) *J. Math. Phys.*, **18**, 756.
- [105] M. Field, et. al, (1993) *Phys. Rev. Lett.*, **70**, 1311.
- [106] S. A. Gurvitz, (1997) *Phys. Rev. B*, **56**, 15215.
- [107] M. Hillery and M. O. Scully, in *Quantum Optics, Experimental Gravitation and Measurement Theory*, Eds. P. Meyestse and M. O. Scully (Plenum, New York, 1983), p. 65.
- [108] M. O. Scully, B. J. Englert and H. Walther, (1991) *Nature* (London), **351**, 111.
- [109] P. G. Kwiat, A. M. Steinberg and R. Y. Chiao, (1994) *Phys. Rev. A*, **49**, 61.
- [110] H. Ohno, et. al., (2000) *Nature* (London), **408**, 944.